Cell sectoring for CDMA cellular systems

SHEN Fangzhong

A Thesis Submitted in Partial Fulfillment of the
Requirements for the Degree of
Master of Philosophy

in

Information Engineering

June 2002

Abstract

Conventional fixed cell sectoring is used to reduce the co-channel interference in 2G wireless systems. However, it is inefficient in addressing hot-spot traffics. Some congested sectors may have outages, while the lightly loaded sectors may have spare capacity. Dynamic cell sectoring, i.e., adaptively changing the sector pattern according to the traffic distribution, can be used to relieve the congestion.

In this thesis, we have systematically studied the dynamic cell sectoring for the Code Division Multiple Access (CDMA) cellular systems from three aspects: Beamforming Networks (BFN), dynamic sectoring algorithms, and Resectoring algorithms.

Circular array is more suitable than linear array for sector beamforming because of its good lobe-shape persistence characteristic. A circular array BFN can produce dynamic sector pattern with the aid of the Butler matrix, which is used to cancel the sidelobe effect.

It is shown that the minimum total transmission power (MinTTP) sectoring scheme can give the optimal sectoring pattern in polynomial time using a shortest path algorithm while suboptimal solution can be found using power equalization (PE) sectoring based on the greedy algorithm with much less computational complexity. The relationship between MinTTP and PE sectoring is discussed under different scenarios. We find that the

total transmission power in a cell using PE Sectoring is very close to that of the MinTTP Sectoring.

When the traffic distribution changes, readjusting the sector pattern is needed. Two resectoring algorithms are proposed and their performance is compared. MinTTP resectoring algorithm has a smaller handoff load than the PE resectoring at the compensation of higher computational complexity.

Thus by installing circular array antennas with a modified BFN and adding a dynamic sectoring controlling module to a conventional fixed sectoring base station, hot-spot congestions in a cell can be relieved.

摘要

近年来基于无线传输的数据和语音业务的不断增长促使无线通信系统的容量的短缺。如何有效地提高系统的容量是近年来研究的热门课题。码分多路（CDMA)是一代通信系统的主流空中接口技术，它的系统容量基于系统的干扰。降低系统干扰就可以有效地提高系统的容量。利用定向天线把一个小区分成若干个扇区（Sectoring）是其中一种降低同道干扰的方法。然而如果一个小区里用户的分布很不均匀，将会导致某些扇区因为拥塞而导致用户服务质量的下降，同时另外一些扇区很可能非常空闲。能否把那些闲置的资源利用起来是本文研究的课题。

通过根据小区用户的分布而动态地调整各扇区的大小和位置，消除各个扇区用户分布失衡的情况，从而达到增加系统容量的目的，我们称这种技术为动态扇区划分。本论文从（1）如何实现动态扇区覆盖，（2）动态扇区划分算法，和（3）动态扇区划分更新算法三个方面系统地研究这种技术。

环形天线阵列比线性天线阵列更加适合各个扇区的波束形成，因为前者生成的波束在转动时形状失真小于后者。利用环形天线阵列和巴特勒矩阵我们提出了一种能够产生动态扇区覆盖的波束形成网络结构。

接下来，本文研究了基于最短路径算法可以在多项式时间内得出最优解的最小发射能量分扇区算法（MinTTP Sectoing），和基于贪婪算法的能量均衡分扇区算法（PE Sectoring）。并且讨论了两者间的内在联系，后者在若干迭代之后可以近似收敛到前者的解。后者因为计算复杂度小，更适合实时的操作。

最后，我们讨论了关于如何分时监测小区内的用户变化从而适当地更新动态分扇区的问题。

通过改造原有的天线阵列结构，加入动态扇区控制模块和波束形成网络模块，传统的基站可以在用户分布不均时提供更多的系统容量。

Acknowledgements

Being at the end of my two-year postgraduate study, I have a lot of thanks to many people.

First, I am truly indebted to professor Tak-shing Peter Yum, my supervisor, for his support and guidance throughout these two years. I am proud to be educated by such an innovative thinker who has an outstanding research discipline and deepest insight to interesting research problems. I am especially impressed by his willingness and generosity in sharing his wisdom with me and all his students. Moreover, I benefit a lot from him more than research. It has been a genuine pleasure to have professor Yum as my supervisor.

I would like to express my gratitude to Dr. Yang Yang, who shares his research experience with me, and help me a lot in daily life. I would like to thank Dr. Li Qiang, Mr. Hua Cunqing for their enjoyable discussions. I would like to thank K.T. Chan for his support in computer maintenance. I would like to thank all graduates at Comtech Lab for their friendship and fun.

I am thankful to my parents, and my elder brother for their love and continuous support. I am thankful to all my teachers, past and present. Without their guidance, I will not be here today. Finally, I would thank my dear girl friend Ms. Yu Yiting, for her love, encouragement and understanding.

Table of Contents

List of Figures

List of Tables

Chapter 1. Introduction

1.1. Motivation

High capacity is needed for the growing wireless services. Code Division Multiple Access (CDMA)[20-23][34] is an access scheme that can provide flexible high capacity. Because CDMA systems are interference limited, we can achieve extra capacity through reducing the system interference. There are a lot of techniques that can be used to mitigate the interference, one of which is the cell sectoring [19-21].

Cell sectoring is used to increase the cellular system capacity through reducing the co-channel interference. Traditional sectoring is fixed sectoring with 3 or 6 sectors and identical sector size. It is efficient to mitigate the interference in case of uniform traffic in a cell. However, when the cell has nonuniform traffic but is using uniform fixed sectoring, some sectors may suffer from heavy congestion, while the others may have spare capacity.

By using Smart Antenna (SA), each beam can track a particular user. Thus the interference from other users cannot affect the desired user. However this approach also increases system complexity.

We make a trade-off between the performance and complexity. We would think why not steer the sector boundaries to split the hotspot and share the high load among the sectors. In this way, the interference can be dynamically reduced, while the beamforming complexity is not so high. This technique is called ***Dynamic cell Sectoring (DS)***.

1.2. Related Work

In [3][4][6] the authors introduced the idea of DS and proposed various heuristic DS algorithms. In a recent study [7], an optimal uplink (from the mobile station to the base station) DS algorithm was given for both receive power optimization and transmission power (TP) optimization, aiming to enhance the uplink capacity.

1.3. Our Work

We focus on the downlink (from the base station to the mobile station) capacity enhancement, and systematically analyze the DS algorithms and their internal relationships. Finally, we propose resectoring (sectoring update) algorithms to make the above DS algorithms perform smoothly with time-varying traffic, i.e., we frequently update the sectoring pattern to ensure the optimality of the sectorization all the time. The term "optimality" will be elaborated in chapter 3.

1.4. Some Assumptions

This section describes the assumptions of this thesis.

1.4.1. Beamforming

For simplicity, we assume each sector is covered by a fan-shape beam, and there is no overlap between any two sectors. The inter-sector interference thus can be neglected.

1.4.2. Downlink Channel

For data services, the downlink traffic will be higher than the uplink traffic in most cases. Thus the downlink capacity enhancement is of practical importance for wireless data services. We will focus on the downlink in this thesis.

1.4.3. Single Cell

We only consider the single cell case. For multi-cell cases, we can modify the analysis by adding the outer-cell interference.

1.5. Thesis Road Map

The thesis is organized as follows. In chapter 2, we will have a review on the cell sectoring techniques and the principles of antenna arrays. A circular array BFN can produce dynamic sector patterns with the aid of the Butler matrix, which is used to cancel the sidelobe effect. Power control as a critical technique in CDMA radio resource management will be discussed in the downlink. Chapter 3 describes two dynamic sectoring schemes. MinTTP Sectoring based on the shortest path algorithm obtains the optimal solution in polynomial time, while the PE sectoring, which based on the greedy algorithm can converge to the optimal solution with much less computational complexity. We conduct the performance evaluation of the two sectoring schemes based on computer. In chapter 4, we develope the resectoring algorithms and finally we conclude our work and show the future work in chapter 5.

Chapter 2. Preliminaries of Cell Sectoring

2.1. Introduction

CDMA cellular systems typically employ universal frequency reuse, where the bandwidth is shared by all the cells. One of the simplest methods for controlling co-channel interference (CCI) is to use directional antennas at the base station (BS). On the downlink channel, directional antennas reduce the generation of CCI by transmitting the signals to the mobile stations (MS) with a narrower beam compared with that of the omni-directional antennas.

There are a lot of beamforming methods to form the beams to cover the cell sectors. Two most common antenna array techniques are Linear Array and Circular Array [13-14][31-32].

2.2. Beamforming

We only consider the base station side. The BS installs multi-antennas to form directional beams. The signals are fed to BeamForming Network (BFN). By controlling the weight matrix of the BFN, the main lobe can be steered to any direction it desires. It is the principle of adaptive antennas. If we calculate the weight matrix in advance, the BFN can provide fixed beamforming. This method is adopted in the traditional fixed sectoring systems.

It is the same in the uplink when using the multi-antennas to receive a signal from a particular direction, since both links are symmetrical in

beamforming. With the same beam patterns the uplink BFN can also be used to transmit in the downlink.

In an array of identical elements, there are five controls that can be used to shape the overall pattern of the antenna. These are:

- The geometrical configuration of the overall array (linear, circular, planar, spherical, etc.)
- The relative displacement between the elements
- The excitation amplitude of the individual elements
- The excitation phase of the individual elements
- The relative pattern of the individual elements

The simplest and one of the most practical arrays is formed by placing the elements along a line, i.e., linear arrays.

2.2.1. Linear Array

An N-element linear equally spaced antenna array oriented along the x-axis with an element spacing of d is illustrated in Figure 2.1.

For a plane wave incident from direction (θ,ϕ), the difference in phase between the signal component incident on array element m and array element 1 is:

$$\psi_m = km\Delta r = mkd\cos\phi\sin\theta \tag{2.1}$$

where $k = 2\pi/\lambda$ is the *phase propagation factor*. The term λ denotes the wavelength. The array factor is given by

$$f(\theta,\phi) = \sum_{m=0}^{N-1} \omega_m e^{j\psi_m} = \sum_{m=0}^{N-1} \omega_m e^{jmkd\cos\phi\sin\theta} \tag{2.2}$$

By adjusting the set of the weights, $\{\omega_m\}$, it is possible to direct the maximum of the array factor in any desired direction, (θ_0,ϕ_0). Let ω_m be:

$$\omega_m = e^{-jmkd\cos\phi_0\sin\theta_0} \tag{2.3}$$

Then the array factor is:

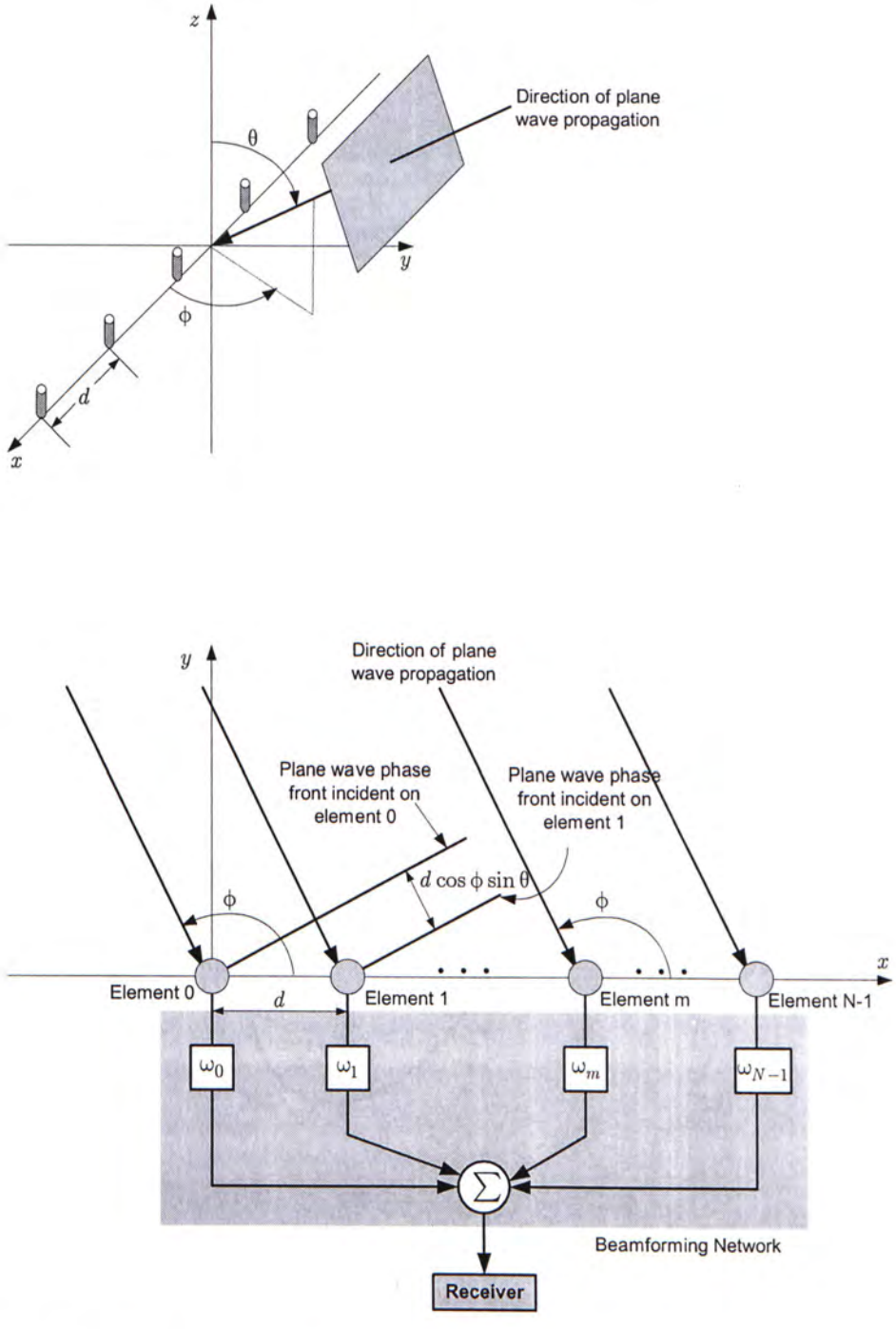

Figure 2.1 A baseband complex envelope model of a linear equally spaced (LES) array oriented along x-axis, receiving a plane wave from direction (θ, ϕ).

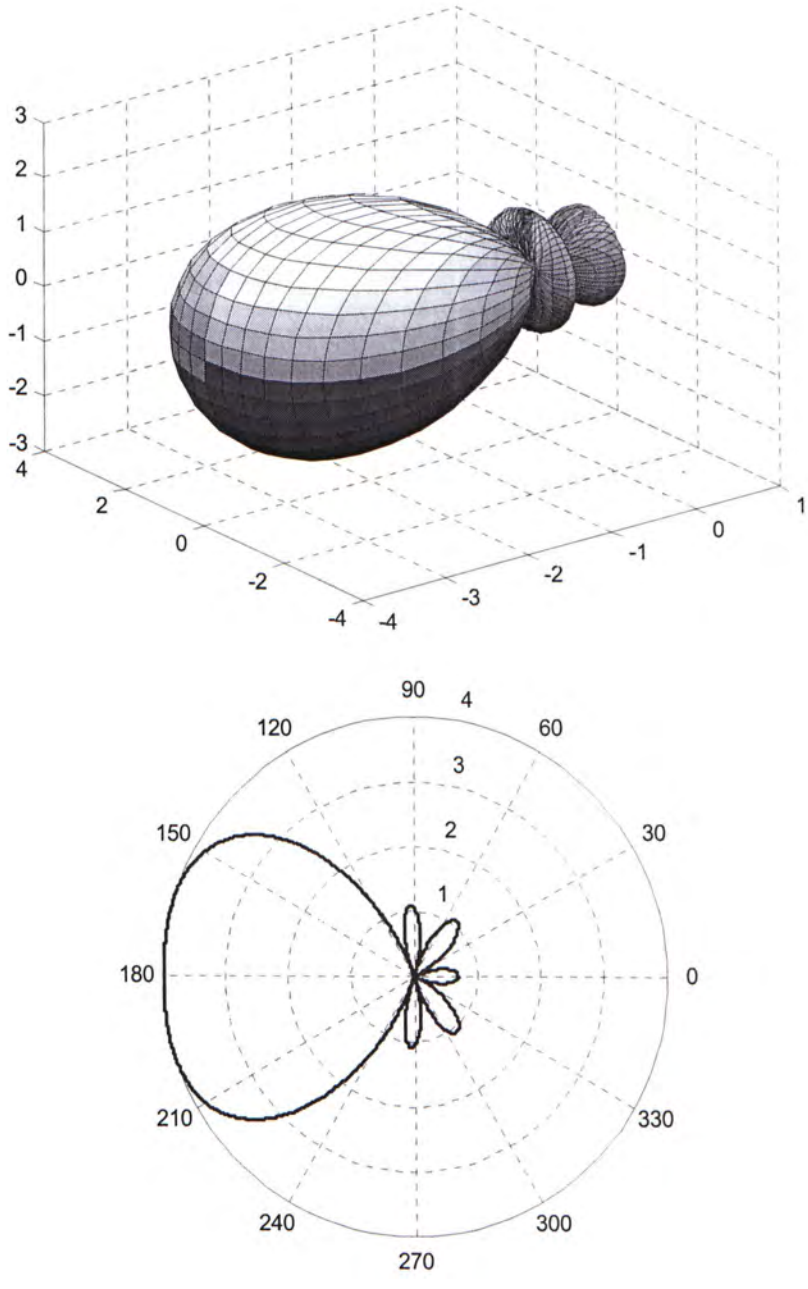

Figure 2.2 Three- and two- dimensional array factor patterns of a 4-element uniform amplitude phased array ($N = 4$, $\beta = -kd\cos\phi_0$, $\phi_0 = 180^\circ$, $d = 2\lambda/5$).

$$f(\theta,\phi) = \sum_{m=0}^{N-1} e^{jmkd(\cos\phi\sin\theta - \cos\phi_0\sin\theta_0)} = \sum_{m=0}^{N-1} e^{jm(kd\cos\phi\sin\theta-\beta)} \tag{2.4}$$

The array factor of 4-element linear equally spaced array is shown in Figure 2.2 for $\phi_0 = 180^\circ$. By varying a single parameter, ϕ_0, the beam can be steered to any desired direction.

2.2.2. Circular Array

A circular array is an array with the elements placed in a circular ring. Referring to Figure 2.3, let us assume that N isotropic elements are equally spaced on the x-y plane along a circular ring of the radius R. IF each array element is fed by a weighted excitation, we can move the main lobe to a desired direction of (θ_0,ϕ_0). The array factor is [32]:

$$f(\theta,\phi) = \sum_{n=1}^{N} e^{jk\rho_0\cos(\phi_n-\xi)} \tag{2.5}$$

where

$$\rho_0 = R\left[\sin^2\theta + \sin^2\theta_0 - 2\sin\theta\sin\theta_0\cos(\phi-\phi_0)\right]^{1/2}$$

$$\xi = \tan^{-1}\left[\frac{\sin\theta\sin\phi - \sin\theta_0\sin\phi_0}{\sin\theta\cos\phi - \sin\theta_0\cos\phi_0}\right]$$

$$\phi_n = 2\pi\left(\frac{n}{N}\right) = \text{angular position of } n\text{th element on } x\text{ - }y \text{ plane}$$

$$k = 2\pi/\lambda$$

Figure 2.4(b) shows the array factor of an 8-element uniform circular array. The beam pattern of the circular array has very small change when it is steered. It is not the case for linear arrays as shown in Figure 2.4(a), where the beam width and sidelobe level will change a lot in steering. So circular array is much more suitable to produce the subbeams for the dynamic sectoring (this will be addressed in section 2.2.4).

With this feature and by a Butler BFN, the circular array is suitable to produce the equal size sub-beams. The Butler BFN is a fixed beamforming networks that can produce orthogonal beams. We will discuss the fixed beamforming networks in the following section.

2.2.3. Butler Beamforming Network

The BFN is characterized by a weight matrix $\mathbf{T}$, where the vector of signals at the output of the matrix, $\mathbf{y}(t)$, is related to the vector of signals at the BFN input, $\mathbf{s}(t)$, by

$$\mathbf{y}(t) = \mathbf{T}^H \mathbf{s}(t) \tag{2.6}$$

The n^{th} output of the BFN corresponds to an array weight vector contained in the n^{th} column of $\mathbf{T}$. Often, a beamforming network is used to produce N beams from N elements. The $N \times N$ BFN Matrix is given by:

$$\mathbf{T} = \begin{bmatrix} \mathbf{w}_0 & \mathbf{w}_1 & \cdots & \mathbf{w}_{N-1} \end{bmatrix} \tag{2.7}$$

The beams are orthogonal if the weight vector corresponding to each beam is orthogonal to those of other beams. Butler matrix can be used to produce those orthogonal beams. The structure of the Butler matrix is shown in Figure 2.5(a). It can be easily shown that the weight vectors corresponding to each port in Table 2.1 are mutually orthogonal. Beam patterns for a larger 8×8 beamforming network matrix are shown in Figure 2.5(b).

Table 2.1 Element phasing, beam direction, and inter-element phasing for Butler matrix of Figure 2.5(a).

	Element 1	Element 2	Element 3	Element 4	Beam Direction	Inter-Element Phasing
Port 1	$-45°$	$-180°$	$45°$	$-90°$	$138.6°$	$-135°$
Port 2	$0°$	$-45°$	$-90°$	$-135°$	$104.5°$	$-45°$
Port 3	$-135°$	$-90°$	$-45°$	$0°$	$75.5°$	$45°$
Port 4	$-90°$	$-45°$	$-180°$	$-45°$	$41.4°$	$135°$

2.2.4. Dynamic Beamforming

Figure 2.6 shows the structure of dynamic beamforming, where the Butler matrix is structured to orthogonalize the subbeams so as to minimize the sidelobe effect. The beamforming network contains the weight matrix responsible for producing N subbeams. The reason for producing N subbeams from N array elements is to ensure that the BFN can generate the mainlobe to its desired user, while at the same time null out the *N-1* interferers (N array elements adaptive antenna has the capability of tracking N users at a time). In this thesis, it is for the sidelobe cancellation. Note that the sidelobes cannot be cancelled for L beams with less than L array elements with a Butler matrix.

With the circular array, the BFN can generate N subbeams with identical beam widths of angular spacing $2\pi/N$. Figure 2.7 gives an illustration of six non-equal sectors by combining subbeams. The BFN matrix and Butler matrix are bi-directional, which means that each subbeam port corresponding to a particular transmit beam pattern can also be used to receive, using the same beam pattern.

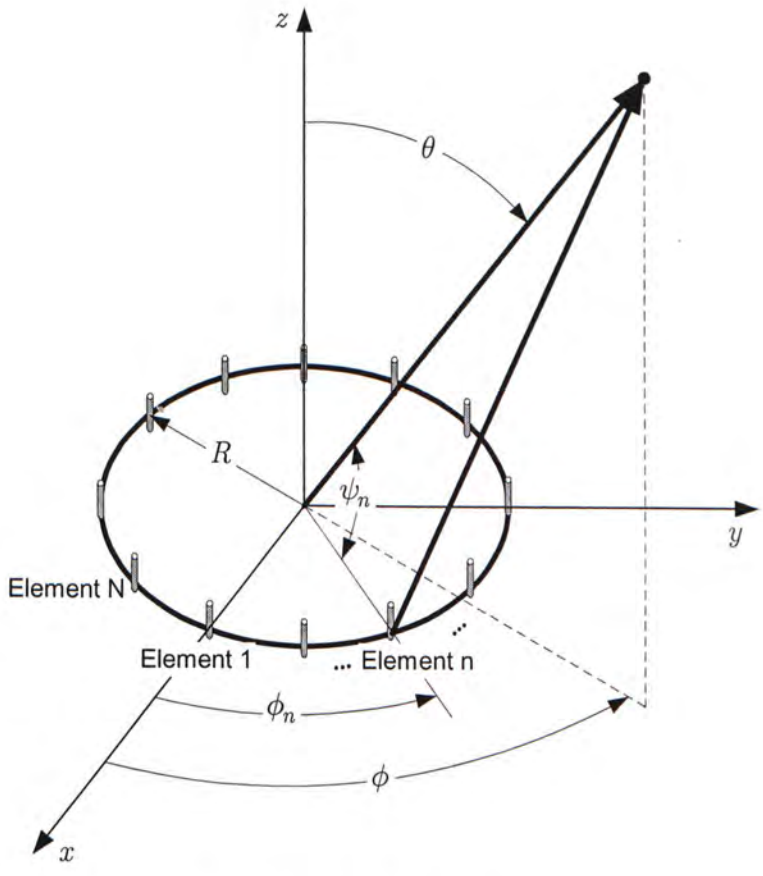

Figure 2.3 Geometry of an *N*-Element circular array.

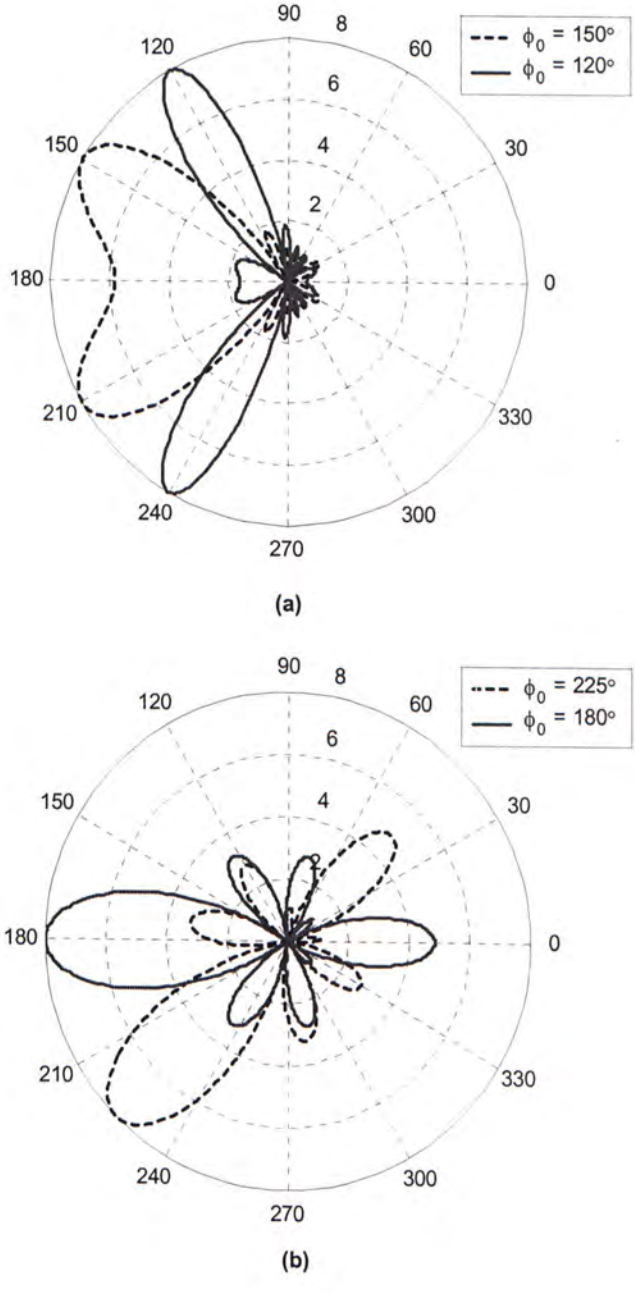

Figure 2.4 (a). Array factor patterns of an 8-element uniform linear phased array ($N = 8$, $\phi_0 = 120^\circ$ and 150° , $d = 0.4\lambda$). (b). Array factor patterns of an 8-element uniform circular phased array ($N = 8$, $\phi_0 = 180^\circ$ and 225° , $kR = 8$).

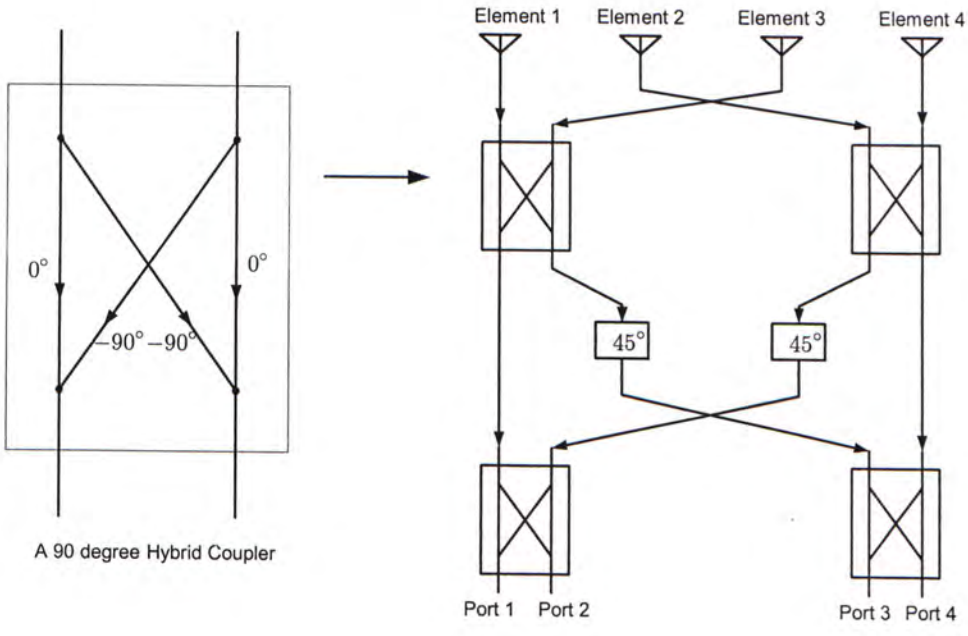

(a)

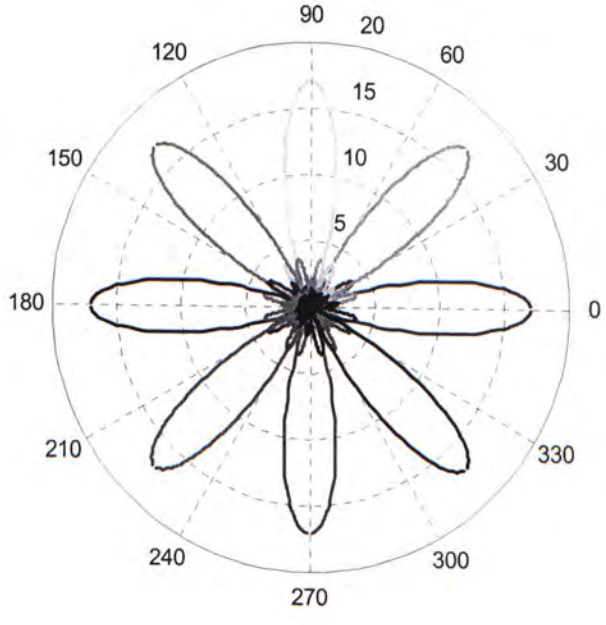

(b)

Figure 2.5 (a) A Butler matrix for fixed beamforming. (b) A set of 8 orthogonal beams is produced using butler matrix. Note that the maximum of each pattern corresponds to the nulls of the other beams.

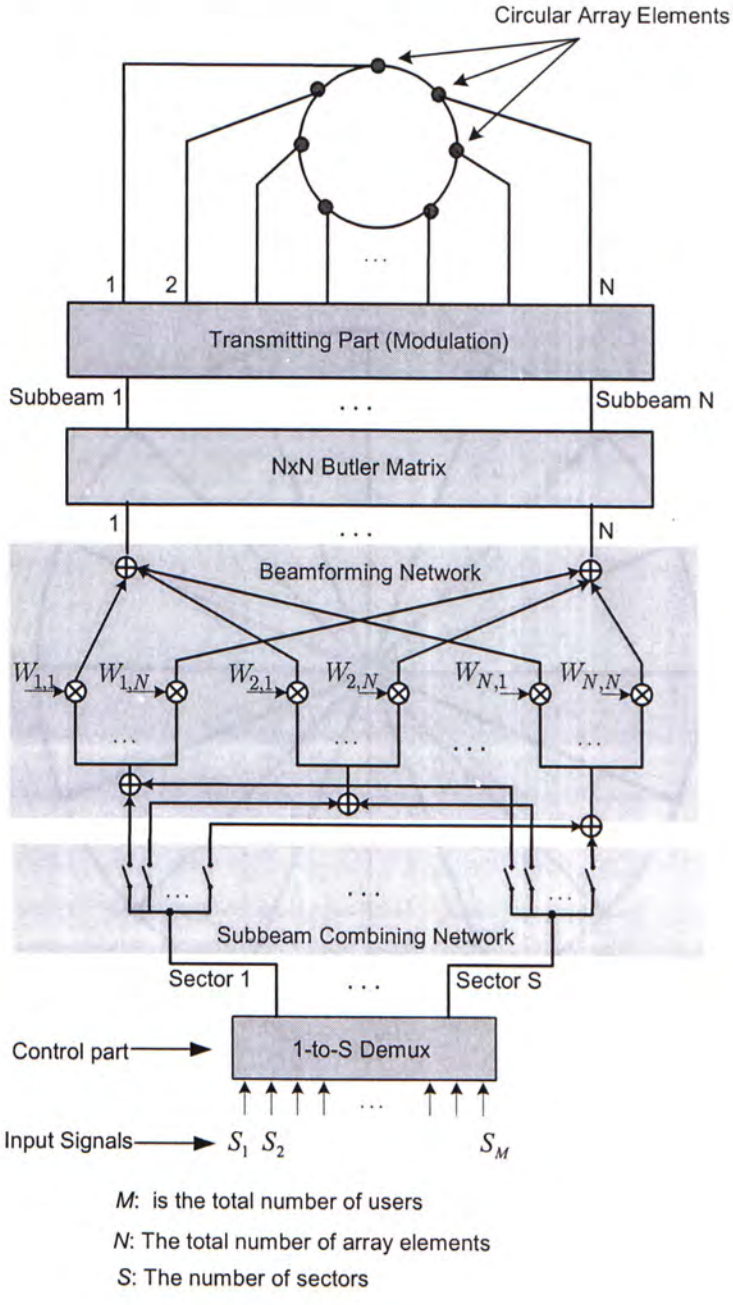

Figure 2.6 Block diagram of transmitting beamforming for a dynamic sectoring system: The input signals are selected to different sectors by the 1-to-S de-multiplexer; The subbeam combining network is responsible to choose the continuous subbeams to form the sectors. The beamforming network produces N subbeams with angular distance of $2\pi/N$. The Butler matrix is used to form orthogonal beams, such that the sidelobe effect is minimized. Finally the weighted input signals are modulated to RF and fed to the circular array.

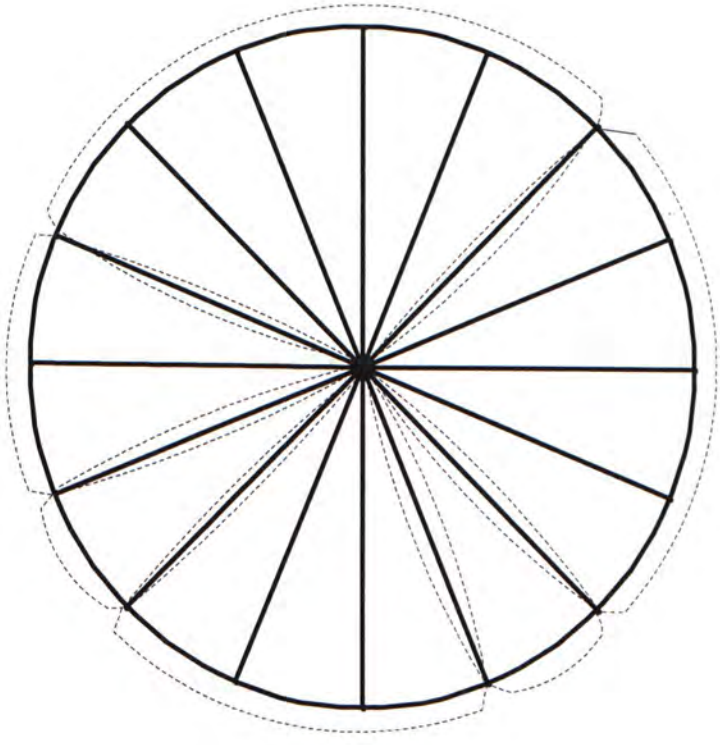

Figure 2.7 Illustration of producing six non-equal sectors by combining subbeams.

2.3. Power Control

Power control is a crucial part of radio resource management for CDMA cellular systems. Optimal power control means that each user receives and transmits just enough to properly convey information with minimum interference to other users. In this thesis, perfect power control is assumed in the downlink, i.e., every mobile station in the cell receives exactly its desired Signal to Interference Ratio (SIR) level. Figure 2.8 shows the downlink spatial power control system for a sector. We can see the downlink access is one-to-many (one BS to many MS's) instead of many-to-one as in the uplink. So in the downlink, the desired signal and its interferers are bounded together and experience the same path loss for a particular user. Another difference for the downlink from the uplink is the synchronization. The BS usually receives signals asynchronously from the mobile stations. While in the downlink, synchronization and coherent detection are possible by the use of a common pilot signal. However, due to multipath fading, the orthogonality of the downlink channel will be impaired. Usually micro cellular environments have better orthogonality than the macro cells, due to less severe multipath propagation effect [12].

In [9-11], the transmission power (TP) optimization is regarded as an eigenvalue problem while neglecting the thermal noise effect. For a sectorized single cell, there are fewer users in a sector than in a cell and if only single cell case is considered, there is no outer-cell interference. Thus thermal noise effect cannot be ignored.

The minimum transmission power for user i is determined by the spectrum bandwidth W, data rate R_i, path gain h_i, noise power level P_N, voice activity factor (VAF) v_i, and orthogonality factor (ORF) α_i. Here α_i is a value between $[0,1]$, where 0 means perfectly orthogonal and 1 means non-orthogonal. Assume there are K users in a sector. The signal to interference ratio can be expressed as follows:

$$\rho_i = SIR_i = \frac{p_i h_i W/R_i}{\alpha_i \sum_{j\neq i, j=1}^{K} (p_j v_j) h_i + P_N} = \frac{p_i W/R_i}{\alpha_i \sum_{j\neq i, j=1}^{K} (p_j v_j) + P_N / h_i}. \qquad i = 1, \cdots, K \tag{2.8}$$

We can calculate the p_i in the above equations in a matrix form:

$$\begin{pmatrix} W/R_1 & -\alpha_1 v_2 \rho_1 & \cdots & -\alpha_1 v_K \rho_1 \\ -\alpha_2 v_1 \rho_2 & W/R_2 & \cdots & -\alpha_2 v_K \rho_2 \\ \vdots & & \ddots & \vdots \\ -\alpha_K v_1 \rho_K & -\alpha_K v_2 \rho_K & \cdots & W/R_K \end{pmatrix} \begin{pmatrix} p_1 \\ p_2 \\ \vdots \\ p_K \end{pmatrix} = \begin{pmatrix} \rho_1 P_N / h_1 \\ \rho_2 P_N / h_2 \\ \vdots \\ \rho_K P_N / h_K \end{pmatrix} \tag{2.9}$$

Rewrite expression (2.9) as $\mathbf{AP} = \mathbf{b}$. If we further assume all the users have the same orthogonality factor, VAF, the same data rate (single service) and the same desired SIR level, $\mathbf{A}$ can be rewritten into:

$$\mathbf{A} = \begin{pmatrix} W/R & -\alpha v \rho & \cdots & -\alpha v \rho \\ -\alpha v \rho & W/R & \cdots & -\alpha v \rho \\ \vdots & & \ddots & \vdots \\ -\alpha v \rho & -\alpha v \rho & \cdots & W/R \end{pmatrix}_{K \times K} \tag{2.10}$$

In (2.10) $\mathbf{A}$ has only two eigenvalues: one is *K-1* duplicated eigenvalue $W/R + \alpha v \rho$, and the other is $W/R - (K-1)\alpha v \rho$. Since the power vector must be all positive, $W/R - (K-1)\alpha v \rho$ should be positive, which can be expressed as:

$$K < \frac{W}{R} \cdot \frac{1}{\alpha v \rho} + 1 \tag{2.11}$$

The term W/R in the above equation is called *processing gain* and denoted as G, which is different from *spreading factor* [23]. The spreading factor usually is the PN code length. The processing gain for IS-95 [23] systems results from a combination of PN-spreading and convolutional coding. For IS-95 systems, there are a total of 64 codes for a sector or a cell. Excluded one pilot channel, one paging channel and one synchronous channel, there

are 61 data traffic channels left for a single carrier. Here K must be smaller than 61 in this example. Usually K is at most between 12 to 15 for IS-95 systems.

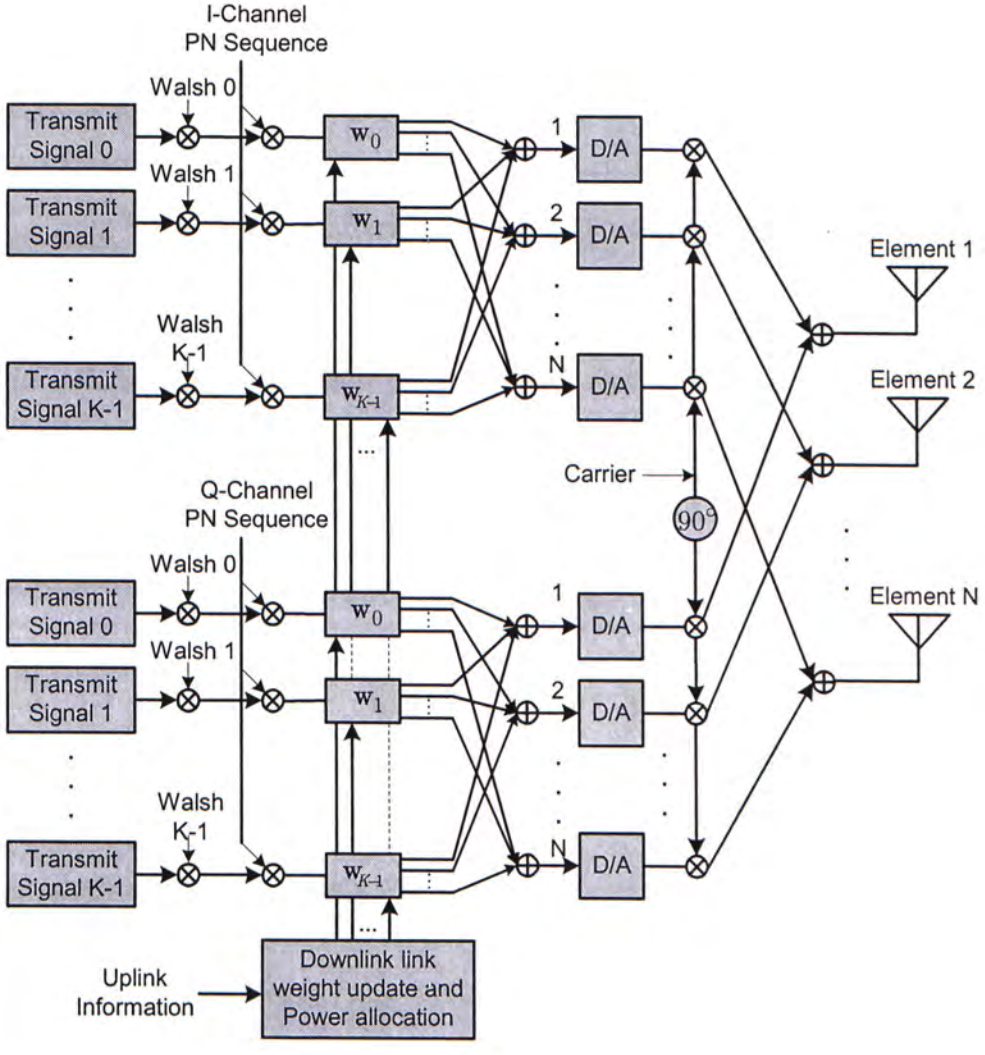

Figure 2.8 A CDMA downlink spatial power control system.

Chapter 3. Dynamic Cell Sectoring

3.1. Introduction

Cell Sectoring is used to increase the cellular system capacity through reducing the co-channel interference. Traditional Sectoring is fixed sectoring with 3 or 6 sectors and equal sector size. When the cell traffic is nonuniform, there will be some sectors suffering from highly congested traffic load, while the others may have spare capacity. A steerable sectoring can solve this problem as shown in Figure 3.1.

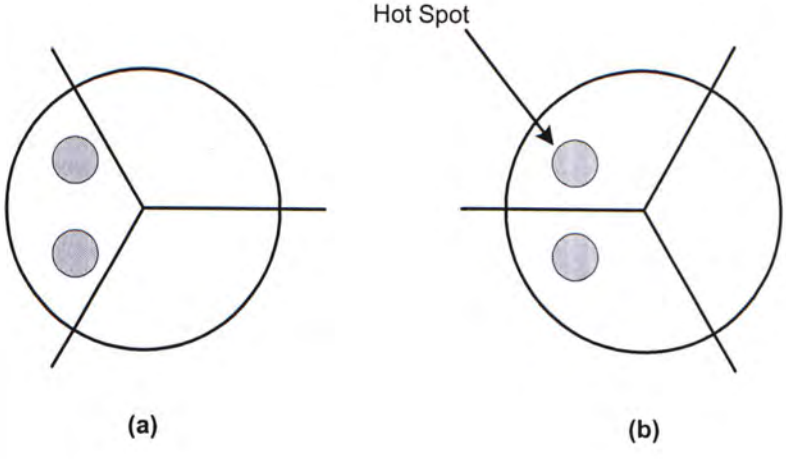

Figure 3.1 (a) Fixed sectoring; (b) Steerable fixed sectoring.

With more sophisticated beamforming techniques (like software radio [1] or a Butler matrix fed circular array we addressed in section 2.2.4), we can dynamically change the sector size to maximize the system capacity. Figure 3.2(c) shows the idea of dynamic sectoring by balancing the load among existing sectors.

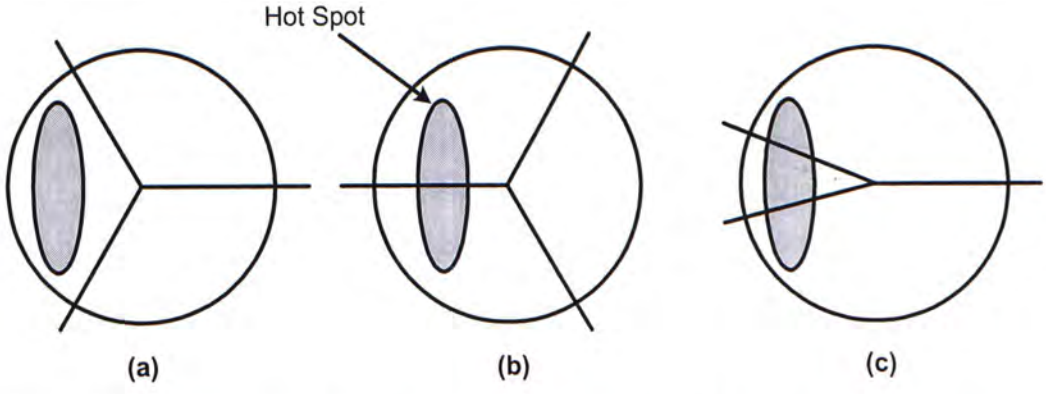

Figure 3.2 Dynamic cell sectoring illustration: (a) fixed sectoring; (b) steerable fixed sectoring; (c) dynamic sectoring.

We can dynamically sectorize the cell based on the following criterions:

(a) Minimum total transmission Power (*MinTTP*)

(b) Sector Load Equalization

- Power Equalization (*PE*)
- User size Equalization (UE)

MinTTP Sectoring: Assuming perfect power control, we can obtain identical SIR level for all mobile users. Based on this assumption, we dynamically sectorize the cell to achieve the minimum TTP. This method is optimal in terms of getting the maximum system capacity, since it reduced the system interference most. The downlink system load can be represented by the transmission power, throughput and number of links. So downlink load balancing can be power balancing, throughput balancing or active user

size balancing. If only voice traffic is considered, the throughput balancing is the same as active user balancing.

PE Sectoring: By equalizing the power among sectors, the interference is also equalized. Thus outage probability is reduced and the capacity increased. Outage probability is the possibility of a user losing its service during a call. This method also benefits its neighboring cells although the multi-cell is not considered here. By mathematical analysis and simulation observation, MinTTP sectoring and PE sectoring have close relationship to each other, and we will address this part at the section 3.3.1. MinTTP sectoring needs centralized control, while the PE sectoring can be either centralized or distributed. For distributed cell sectoring, the computational complexity is often much lower than the centralized sectoring algorithms.

UE sectoring: This means steering the sector boundaries to have equal users in each sector. In some uniform traffic situations it can perform fairly well. Also this method can be performed in centralized or distributed way.

3.2. Minimum Total Transmission Power sectoring

3.2.1. Problem Statement

We first consider the optimization problem of minimizing the total transmission power at the base station by choosing the transmission power for each user and sector partition patterns.

The transmission power optimization problem can be expressed as

$$\begin{aligned}
&\min_{\Theta,\mathbf{p}} \sum_{k=1}^{S} \sum_{i\in X_k(\Theta)} p_i \\
&\text{subject to } SIR_i = \frac{Gp_ih_i}{\alpha_i\sum_{j\neq i}\left(\delta_{ij}p_jv_j\right)h_i + P_N} > SIR^t. \quad i = 1,\cdots,M \\
&\qquad \mathbf{p} \geq 0, \qquad \mathbf{p} = (p_1,\cdots,p_M) \\
&\qquad \textstyle\sum_{k=1}^{S}\theta_k = 2\pi, \qquad \Theta=(\theta_1,\cdots,\theta_S)
\end{aligned} \tag{3.1}$$

where

$X_k(\Theta)$: User indices set for sector k

$\Theta = (\theta_1,\cdots,\theta_S)$: Sector size vector

$$\delta_{ij} = \begin{cases} 1, & \text{if } i \in X_k(\Theta) \text{ then } j \in X_k(\Theta). \\ 0, & \text{otherwise.} \end{cases}$$

v_i : Voice activity factor

α_i : Orthogonality factor

h_i : Path gain for user i

S : Number of sectors

$M_k = \left|X_k(\Theta)\right|$: Number of users in sector k

G : Processing gain

P_N : Thermal noise power

SIR^t : Required signal-to-interference ratio

We can calculate p_i in a sector by solving equation(2.9). For simplicity, we assume identical Voice Activity Factor (VAF) α , ORthogonal Factor (ORF) v and required SIR level ρ for all users. Then we add p_i together to obtain the transmission power P_k for sector k :

$$P_k = \sum_{i\in X_k(\Theta)} p_i = \frac{\rho P_N}{G-\left(M_k(\Theta)-1\right)B}\sum_{i\in X_k(\Theta)}\frac{1}{h_i}, \quad k = 1,\cdots,S \tag{3.2}$$

where $B = \alpha v\rho$. The total transmission power in the cell is:

$$TTP = \sum_{k=1}^{S} P_k = \sum_{k=1}^{S} \frac{\rho P_N / B}{(G/B+1) - M_k(\Theta)} \sum_{i \in X_k(\Theta)} \frac{1}{h_i} \tag{3.3}$$

From (2.11), we know that the number of users in a sector must be smaller than $\frac{W}{R} \cdot \frac{1}{\alpha v \rho} + 1$, i.e., $M_k < G/B + 1, \forall k$. Therefore the optimization problem (3.1) can be replaced as

$$\begin{aligned} &\min_{\Theta, M_k} \sum_{k=1}^{S} \frac{\rho P_N / B}{(G/B+1) - M_k(\Theta)} \sum_{i \in X_k(\Theta)} \frac{1}{h_i} \\ &\text{subject to } M_k < G/B + 1, \quad \sum_{k=1}^{S} M_k = M \\ &\qquad \sum_{k=1}^{S} \theta_k = 2\pi, \quad \Theta = (\theta_1, \cdots, \theta_S) \end{aligned} \tag{3.4}$$

This is an NP-hard optimization problem if we search all the possible sectoring patterns to find the optimal one. In the following section, we show how we formulate this problem into a shortest path problem. A modified Dijkstra's algorithm is introduced, and in a polynomial time $O(M^3 S)$ we find the optimal solution.

3.2.2. Shortest Path Problem Formulation

In [7], Saraydar and Yener modeled the uplink transmit power optimization problem as a shortest path problem. Here, we use the same method to formulate the power optimization problem in the downlink.

Figure 3.3 shows us the three steps of converting the sectoring problem into the shortest path problem. They are:

1. Construct a ring based on user locations. Extend the position of the mobile stations onto the ring, and a mobile is replaced by a node on the ring. We thus obtain a ring with M nodes.
2. Select a reference edge on the ring. Remove the edge and transfer the ring into a string with M nodes.
3. Partition the M nodes on the string into S subsets. List all the possible partition patterns in a network.

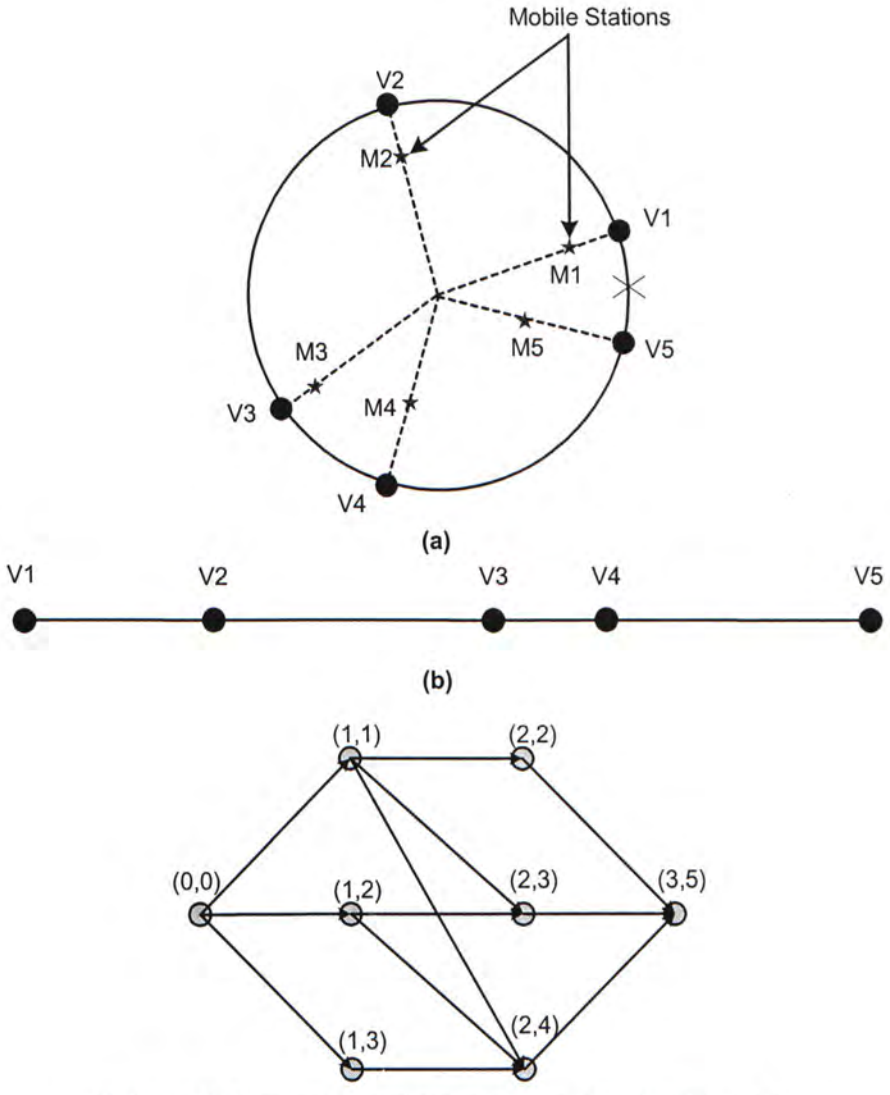

(0,0) and (3,5) are respectively the source and destination nodes.
The nodes lie between them are given by the set:

$$\{(i,j): 1 \leq i \leq S-1; i \leq j \leq M-S+i\}$$

where S is the number of sectors, M is the number of users in the cell.

(c)

Figure 3.3 (a) Construct a ring based on the user locations. (b) Remove the ring edge between V1 and V5, and obtain a string with 5 nodes. (c) A network constructed from a string that is to be partitioned into 3 subsets.

In the following we generalize the example. The corresponding shortest path algorithm is developed and analyzed in Section 3.2.3. The problem formulation in this section is based on [7].

Given a graph $G=(V,E)$, let $\pi=\{X_1,\cdots,X_S\}$ be a *partition* of the set of vertices V into S subsets. π is considered feasible when $X_k \neq \varnothing$, for all k. The set of all such feasible partitions is denoted by $\prod(G,S)$. The cost function $C:\prod(G,S)\rightarrow \Re$ assigns a value to each feasible partition and the cost of a particular partition $\pi=\{X_1,\cdots,X_S\}$ is given by

$$C(\pi)=\sum_{k=1}^{S} W(X_k) \tag{3.5}$$

Where the weight $W(X_k)$ of X_k is defined as the sum of the weight of each vertex in X_k. The graph partitioning problem is to find a feasible partition such that the cost is minimized. Mathematically, it can be expressed as

$$\min_{\pi=\{X_1,\cdots,X_S\}}\left\{C(\pi)=\sum_{k=1}^{S} W(X_k)\right\} \tag{3.6}$$

Suppose H is a string with M vertices labeled $v_1,\cdots,v_M$ and with weight of $w_1,\cdots,w_M$. Now we partition these M vertices into S subsets. Suppose that in any feasible partition $\{X_1,\cdots,X_S\}$, the adjacent subsets have consecutive indices. We thus construct an acyclic graph G as follows. Let (0,0) and (S, M) be the source and destination nodes of G, respectively. The nodes that lie between source and destination pair are given by the set

$$\{(i,j): 1\leq i\leq S-1; i\leq j\leq M-S+i\} \tag{3.7}$$

An edge is placed from node (i,j) to (m,n) if m=i+1 and n>j. Otherwise there is no edge between (i,j) and (m,n). There is a one-to-one correspondence between the feasible partitions of H into S subsets and the paths from (0,0) to (S, M) in G. The path P corresponding to a given

$\pi \in \prod(G,S)$ is defined as follows. The node (k,i) belongs to P if and only if i is the last vertex of the subset S_k of π. Furthermore, when the weight of each edge in graph G is assigned the cost of the corresponding subset in H, the cost of partition π, $C(\pi)$ in (3.5) coincides with the total length of path P in network G. It follows that the optimum partition of H can be determined by finding a shortest path from (0,0) to (S, M) in G since each path corresponds to one and only one feasible partition. In Figure 3.3, we show how the graph G is obtained via mapping the original problem of partitioning a cell with 5 mobiles into 3 sectors.

3.2.3. Shortest Path Algorithm and Complexity

A shortest path from the origin to destination can be found by using the well-known shortest path algorithms. As the most famous one, *Dijkstra's algorithm* is used to find the shortest path in a network without negative cyclic edges (i.e., the network must be acyclic or cyclic but no negative edge in the cycle, because otherwise there will be a path with infinitely small value). In the Dijkstra's algorithm, it will EXTRACT (*find and delete then return*) the vertex with minimum d value, and then RELAX (update the d value) [20] (also see appendix in this chapter). However, in our partition problem, the graph is acyclic, and thus Dijkstra's method with a running time of $O\left(V^2 + E\right)$ is not the best way to find the solution. Another shortest path algorithm called *single-source directed acyclic graph* (DAG) *shortest path algorithm* is specifically for those directed and acylic graphs. By *relaxing* (see the RELAX function in the appendix) a weighted DAG $G = (V,E)$ after a topological sort of its vertices, we can compute the shortest path from a single source in $O(V + E)$ time. Fortunately, the graph formulated from a string-partition problem is already sorted. So what we need to do is just to apply the *Breadth-First Search* (BFS) [20] and update the distance values of the nodes on the graph from the source to its destination. The complexity is only $O(E)$.

So for the graphs formulated from the string partition problem, we can use the modified *DAG-Shortest-Paths* (DSP) algorithm. The modified DSP Algorithm for the string partition problem is shown as follows, named *single-source topologically Sorted Directed Acyclic Graph Shortest Paths algorithm (SDAG- SP).*

- **SDAG-SP (G,w,S)**

1. INITIALIZE-SINGLE-SOURCE(G,S)
2. $Q \leftarrow \{S\}$
3. **while** $Q \neq \varnothing$
4. **do** $u \leftarrow head[Q]$
5. **for** each vertex $v \in Adj[u]$ % With $O(E)$ runtime
6. **do** RELAX(u,v,w)
7. ENQUEUE(Q,v)
8. DEQUEUE(Q,u)

Suppose there are totally M mobile stations, S sectors in this optimization problem. We investigate the complexity of *TDAG-Shortest-Paths* algorithm. In Figure 3.4 we can see that except the source and destination nodes, the number of nodes for any column is M-S+1, and there are S-1 columns in the network. Thus

$$V = (M - S + 1)(S - 1) + 2 \tag{3.8}$$

and

$$\begin{aligned} E &= (S-2)\sum_{i=1}^{M-S+1} i + 2(M-S+1) \\ &= (M-S+2)(M-S+1)(S-2)/2 + 2(M-S+1) \end{aligned} \tag{3.9}$$

Therefore

$$O(E) = O\left(M^2 S\right) \text{ where } M \gg S \tag{3.10}$$

The complexity of the SDAG-SP algorithm is $O(M^2S)$ after settle down one reference edge. In addition, the algorithm requires each of the M edges to be a reference edge. Therefore the complexity of the MinTTP Sectoring is $O(M^3S)$.

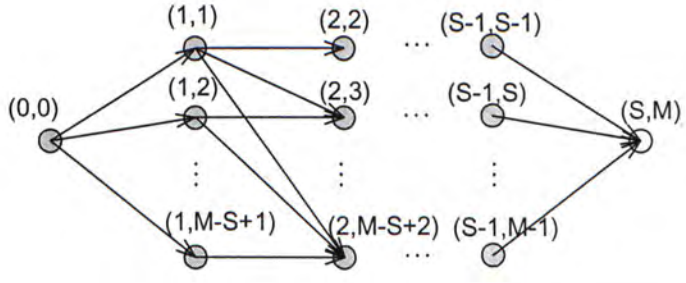

Figure 3.4 A general network for partitioning M nodes into S subsets.

3.2.4. Graph Reduction

Suppose that the solution of the MinTTP Sectoring exists when the users are fairly equalized among sectors (it will be confirmed in section 3.3.1), i.e., those feasible partitions with extremely non-equalized load allocation are almost impossible to be solution candidates and therefore can be deleted. For example, we want to sectorize a cell with 100 users into 3 sectors, we could be quite sure that it is impossible to have a sector with only one user inside. If we delete the paths where an edge contains only one node in the graph G, the total number edges will be reduced by 5.88%. If further we assume that there are at least 10 users in a sector, the total number of edges is reduced by 46.5%. The improvement is significant if we increase the minimum number of users for a sector, however it takes a risk

that it might, though at little possibility, delete the optimal solution. That builds up the trade-cff. Generally, it will not introduce any penalty to this method if we carefully control the value of the minimum number of nodes on an edge, which is denoted as a in the thesis.

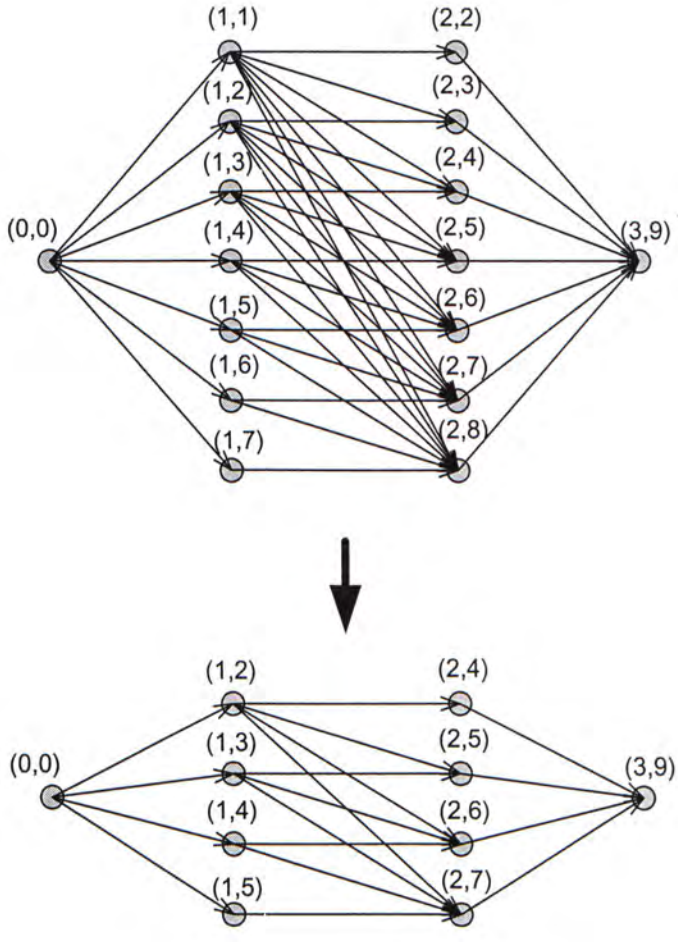

Figure 3.5 Graph reduction after adding the constraint of each edge containing at least two nodes on the string.

After adding this constraint, the number of edges will be decreased from E to E':

$$E' = (S-2)\sum_{i=1}^{M-aS+1} i + 2(M-aS+1) \tag{3.11}$$

$$E = (S-2)\sum_{i=1}^{M-(S-1)} i + 2(M-(S-1)) \tag{3.12}$$

Instead of using the absolute value of minimum number of users, a, we introduce η as the percentage of a over the average number of users in a sector:

$$\eta = \frac{a}{M/S} \tag{3.13}$$

Since a must be smaller than M/S, $0<\eta<1$. Assume $M \gg S$, we can express the reduction ratio of the edges only in terms of η as follows:

$$\frac{E-E'}{E} \approx 1-(1-\eta)^2 = \eta(1-\eta) \tag{3.14}$$

3.2.5. Example

We now use a simple example to illustrate the MinTTP sectoring process. Given the following parameters:

(1) Number of users M: 5

(2) Number of sectors S: 3

(3) $\rho P_N / B$: 1

(4) G/B +:1 4

(5) Path gain vector $\mathbf{h}$: $\left(\frac{1}{3},\frac{1}{2},1,\frac{1}{4},\frac{1}{9}\right)$

1. Initialize the graph, and calculate the edge weights $W(X_k(\Theta))$ for all possible sectoring patterns. Assign zero to the source node and infinity to all of the rest nodes.

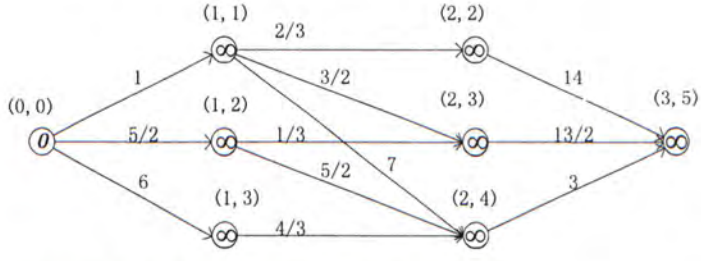

Figure 3.6 Initial Step for the Shortest Path Algorithm.

2. Shortest Path algorithm

Starting from the source node, update its adjacent node values by the RELAX function (see the appendix). Repeat the same process for those adjacent nodes and so on. Once one node updates its value for all the entries and selects the smallest one as its node value, it becomes gray and the corresponding entry will appear as a **bold** line. Finally, the destination node will obtain a smallest node value and a corresponding path from the source node, which gives respectively the minimum TTP and the optimal sectoring pattern for the MinTTP Sectoring problem.

From step 5 in Figure 3.7 we can see the minimum TTP is 8 units, and the corresponding path indicates that the optimal sectoring pattern is ({1 2}, {3 4}, {5}).

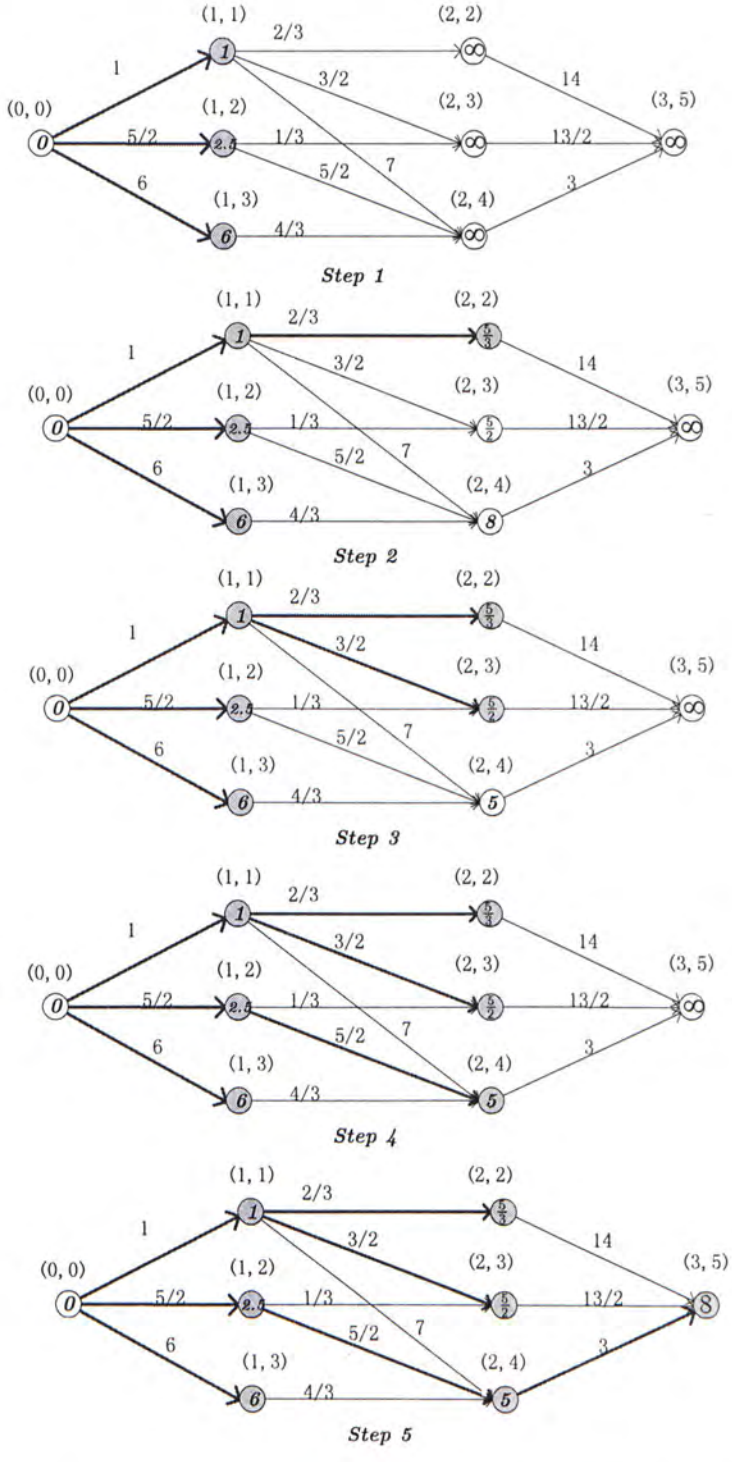

Figure 3.7 The process of the shortest path algorithm in our example.

Let the next ring edge be the reference edge. Repeat the above steps to get the minimum TTP and corresponding sectoring pattern. When M solutions are obtained, choose the one with the minimum TTP as the final solution.

3.3. Power Equalization Sectoring

The optimal sectoring in the downlink is the MinTTP Sectoring, and we obtain the solution via a shortest path algorithm. Compared to the exhaustive search, computational complexity is reduced. However, $O(M^3S)$ complexity is still a challenge for a real time computation. Next, we will discuss the power equalization (PE) sectoring, which is based on the idea to balance the interference among sectors to increase the capacity. PE sectoring can be deployed in a distributed control such that the computational complexity is largely reduced, and real time control therefore is much more practical. We first discuss the relationship between MinTTP sectoring and PE sectoring, and show that both algorithms are equivalent in special cases, and in a general case, the latter one can achieve similar performance as the former one.

3.3.1. Relationship Between MinTTP Sectoring and PE Sectoring

We compare MinTTP and PE Sectoring under three conditions:

1. When $G/B \gg (M_k + 1)$, i.e., when there are very few users in each sector:

$$TTP \approx \frac{\rho P_N}{G} \sum_{i=1}^{M} \frac{1}{h_i} \tag{3.15}$$

   In this case, for whatever partition $X_1(\theta), \cdots, X_S(\theta)$, the TTP will be approximately the same, in other words, no dynamic sectoring is needed.

2. When M_k is comparable to G/B, we first assume $h_i = h$, $\forall i$. The TTP for PE sectoring under this assumption is:

$$TTP_1 = \frac{\rho P_N}{Bh} \frac{\sum_{i=1}^{S} M_i}{(G/B+1) - \frac{\sum_{i=1}^{S} M_i}{S}} \tag{3.16}$$

The TTP for arbitrary sectoring pattern is:

$$TTP_2 = \frac{\rho P_N}{Bh} \sum_{i=1}^{S} \frac{M_i}{(G/B+1) - M_i} \tag{3.17}$$

We observe $TTP_2 \geq TTP_1$. The inequality holds as equality if and only if power in each sector is identical. In other words, MinTTP sectoring is equivalent to PE sectoring at this equal path gain case, which is proved by the following proposition.

Proposition 3.1

$$\sum_{i=1}^{S} \frac{M_i}{Z - M_i} \geq \frac{\sum_{i=1}^{S} M_i}{Z - \frac{\sum_{i=1}^{S} M_i}{S}} \tag{3.18}$$
$$Z > M_i, i = 1, \cdots, S$$

Proof: We use induction method to prove it:

(i) Let $S = 2$

$$left = \frac{M_1}{G - M_1} + \frac{M_2}{G - M_2}$$

$$right = \frac{M_1 + M_2}{G - \frac{M_1 + M_2}{2}}$$

$$left - right = \frac{G(M_1 - M_2)^2/2}{(G - M_1)(G - M_2)\left(G - \frac{M_1 + M_2}{2}\right)} \geq 0$$

left is equal to *right*, if and only if $M_1 = M_2$.

(ii) Suppose when $S = K$, the inequality

$$\sum_{i=1}^{K} \frac{M_i}{Z - M_i} \geq \frac{\sum_{i=1}^{K} M_i}{Z - \frac{\sum_{i=1}^{K} M_i}{K}}$$

is correct. We check when $S = K + 1$, whether the inequality

$$\sum_{i=1}^{K+1} \frac{M_i}{Z - M_i} \geq \frac{\sum_{i=1}^{K+1} M_i}{Z - \frac{\sum_{i=1}^{K+1} M_i}{K+1}} \tag{3.19}$$

is correct or not. Let

$$\sum_{i=1}^{K} M_i = A,$$
$$M_{K+1} = a$$

Then the left of (3.19) is:

$$left = \sum_{i=1}^{K+1} \frac{M_i}{Z - M_i} = \sum_{i=1}^{K} \frac{M_i}{Z - M_i} + \frac{M_{K+1}}{G - M_{K+1}} \geq \frac{A}{G - \frac{A}{K}} + \frac{a}{G - a}$$

The right of (3.19) is:

$$right = \frac{A + a}{G - \frac{A+a}{K+1}}$$

$$left - right \geq \frac{G(A - Ka)^2}{K(K+1)\left(G - \frac{A}{K}\right)(G - a)\left(G - \frac{A+a}{K+1}\right)} \geq 0$$

left is equal to *right*, if and only if $\sum_{i=1}^{K} M_i = KM_{K+1}$.

From (i) and (ii), we conclude that inequality (3.18) is correct, and the equality holds if and only if $M_i = M/S$ for all i. □

3. Next assume $h_j \neq h_k$. We observe by computer simulation the *TTP of PE sectoring* (TTP_{PES}) is similar to *TTP of MinTTP sectoring* (TTP_{MTTPS}) when the square of the users' distance to BS (r^2) is uniformly distributed (the users' angular location distribution can be arbitrary). The simulation result is shown in Figure 3.8 where the y-axis γ is

$$\gamma = \text{Prob}\left(\frac{TTP_{PES} - TTP_{MTTPS}}{TTP_{MTTPS}} < \varepsilon\right) \tag{3.20}$$

From the figure we see both sectoring schemes can achieve similar *TTP* with high probability. Although PE Sectoring is suboptimal in some cases, its computational complexity is much lower than MinTTP Sesctoring.

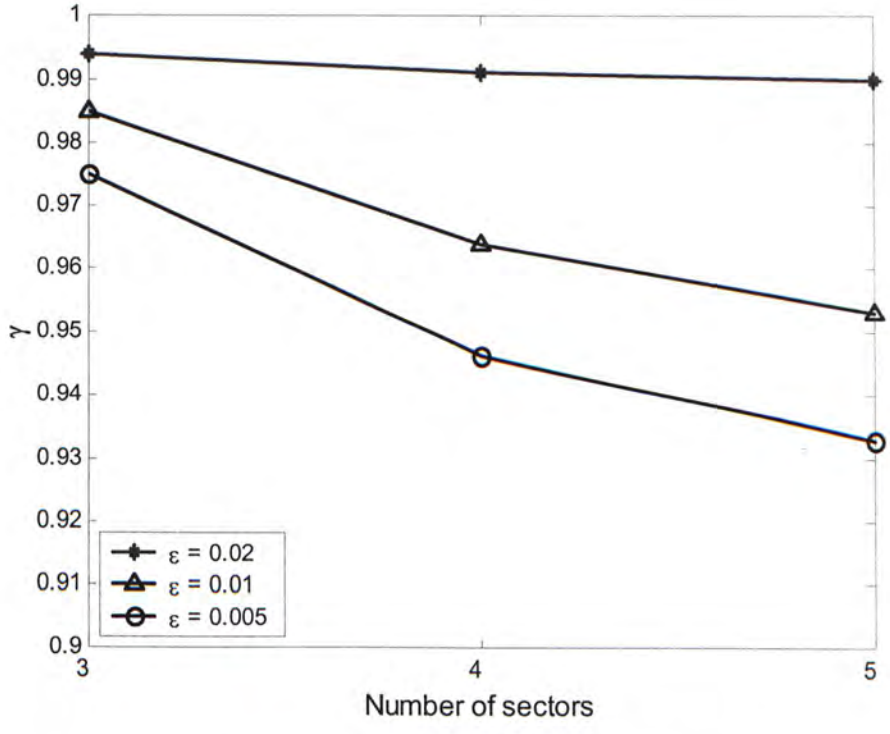

Figure 3.8 Statistic relation between MinTTP Sectoring and PE Sectoring when r^2 is uniformly distributed.

3.3.2. Power Equalization Sectoring Algorithm

MinTTP Sectoring must work under centralized control, whereas the PE Sectoring can work in a distributed way. Each sector boundary controller (SBC) compares the power from its adjacent two sectors, and moves itself to higher power side by handovering one user at a time. Iteratively, the power among sectors will converge to each other.

- ***PES Algorithm***
  1. Select an oriented sector boundary (SB), from which the sectors are labeled counter-clock-wisely (CCW) $1,2,\cdots,S$.
  2. Set $i = 0$.

3. Move the SB between sector i and $i+1$:

$$\begin{aligned} &\text{move SB CCW by one user if } \frac{P_i - P_{i+1}}{P_i} > \xi \\ &\text{move SB CW by one user if } \frac{P_{i+1} - P_i}{P_i} > \xi \qquad i = 1, \cdots, S-1 \end{aligned} \tag{3.21}$$

where $\xi \in (0,1)$ is the threshold.

Otherwise, SB stays still.

4. i increases by 1. If i is smaller than S, go to step 2.
5. Repeat the steps from 2 to 4 till the power is balanced.

3.4. Numerical Results

We provide the results of MinTTP Sectoring, and compare them with the results of PE Sectoring and Fixed Sectoring. Figure 3.9 shows the sector boundaries of the MinTTP Sectoring and Fixed Sectoring in a particular hot-spot scenario. Figure 3.10 shows the sector boundaries in a scenario where the users are uniformly distributed. Figure 3.11 shows the PE sectoring convergence process, where the power in three sectors converge after dozens of iterations; however, if ξ is not properly designed, the convergence will fail, as shown in Figure 3.12. Figure 3.13 shows the TTP comparison for the PE Sectoring and MinTTP Sectoring. We can see the PE sectoring converges its TTP to that of MinTTP Sectoring.

In Table 3.1 and Table 3.2, we give the TTP values of MinTTP Sectoring and Fixed Sectoring at different conditions for the hot-spot scenario shown in Figure 3.9. We see when orthogonality factor increases, the TTP savings of MinTTP Sectoring against FS increase. This shows that MinTTP Sectoring is especially useful in macrocells when the downlink channel orthogonality is impaired a lot. By comparing these two tables, we can see that when the number of users increases, the power savings increase, which shows that MinTTP Sectoring is very useful in congested areas. Furthermore increasing the number of sectors can only help to reduce the TTP on a small scale.

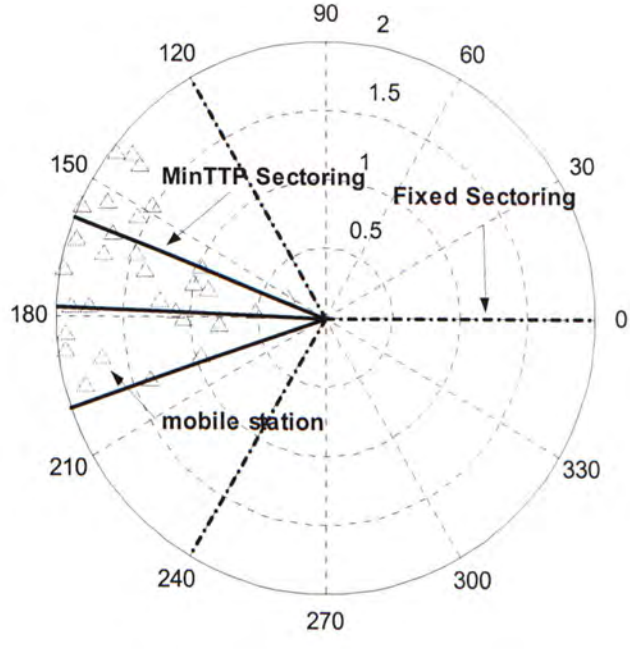

Figure 3.9 Sector boundaries of MinTTP Sectoring and Fixed Sectoring in a cell where the number of mobile stations, $M = 30$, the number of sectors, $S = 3$, the processing gain, $G = 19.3dB$, the target SIR level, $\rho = 8.4dB$, voice activity factor, $v = 0.479$, orthogonality factor, $\alpha = 0.2$, and thermal noise power $P_N = -103dBm$.

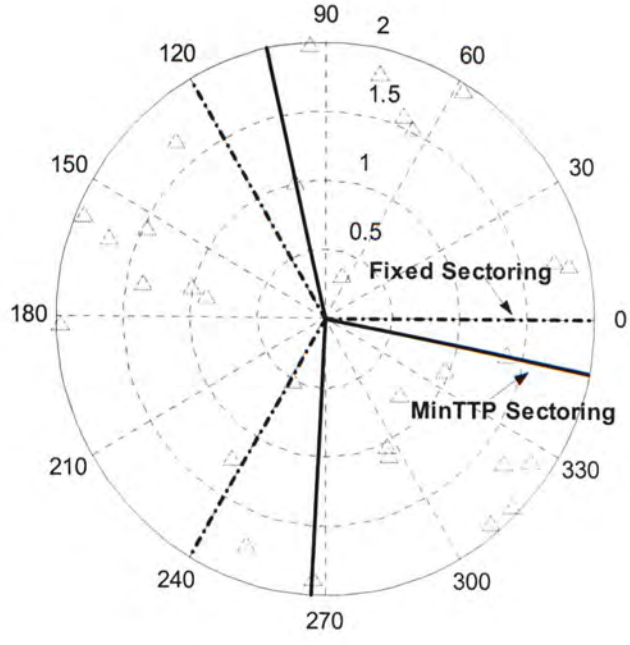

Figure 3.10 Sector boundaries of MinTTP Sectoring and Fixed Sectoring in a cell where the number of mobile stations, $M = 30$, the number of sectors, $S = 3$, the processing gain, $G = 19.3dB$, the target SIR level, $\rho = 8.4dB$, voice activity factor, $v = 0.479$, orthogonality factor, $\alpha = 0.2$, and thermal noise power $P_N = -103dBm$. The distribution of the mobile stations is uniform in the cell.

Table 3.1 Total Transmission Power [Watts] obtained when S=3.

	TTP for MinTTP Sectoring	TTP for Fixed Sectoring	Improvement
$M = 20, \alpha = 0.2$	2.4317	2.7032	10.2%
$M = 30, \alpha = 0.2$	6.1431	7.3182	16.1%
$M = 40, \alpha = 0.2$	7.8899	10.1621	22.4%
$M = 20, \alpha = 0.8$	2.8177	5.3295	47.1%
$M = 30, \alpha = 0.8$	7.9368	-	-
$M = 40, \alpha = 0.8$	-	-	-

Note: '-' means that sectoring is infeasible for the traffic.

Table 3.2 Total Transmission Power [Watts] obtained when S=6.

	TTP for MinTTP Sectoring	TTP for Fixed Sectoring	Improvement
$M = 20, \alpha = 0.2$	2.3645	2.6543	10.9%
$M = 30, \alpha = 0.2$	5.8960	7.1396	17.4%
$M = 40, \alpha = 0.2$	7.4645	9.8715	24.2%
$M = 20, \alpha = 0.8$	2.4865	5.1036	51.3%
$M = 30, \alpha = 0.8$	6.5178	-	-
$M = 40, \alpha = 0.8$	8.8900	-	-

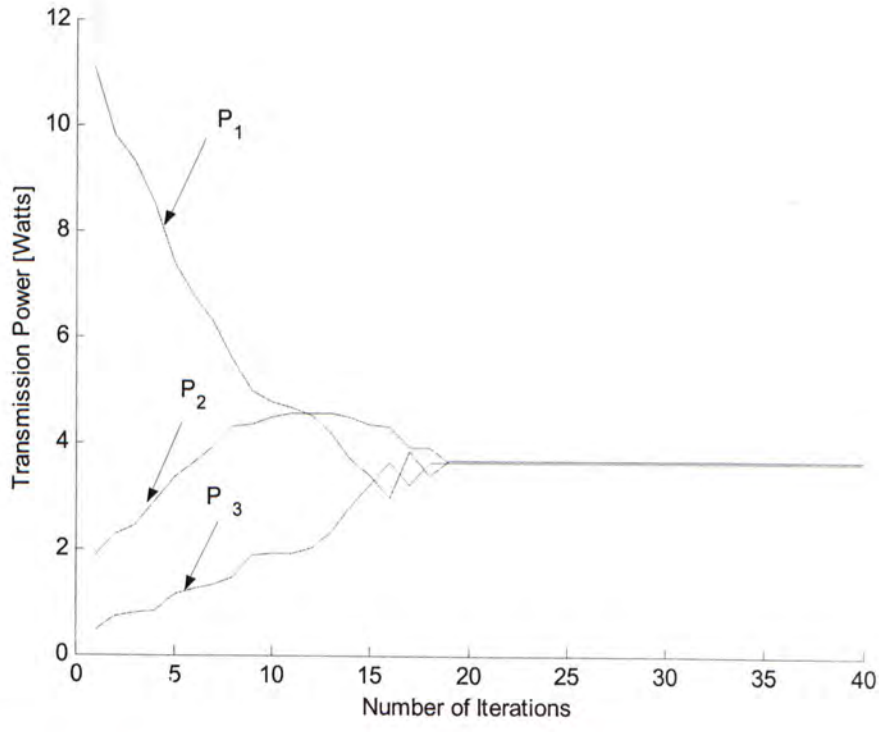

Figure 3.11 The PE Sectoring convergence process when $\xi = 0.02$.

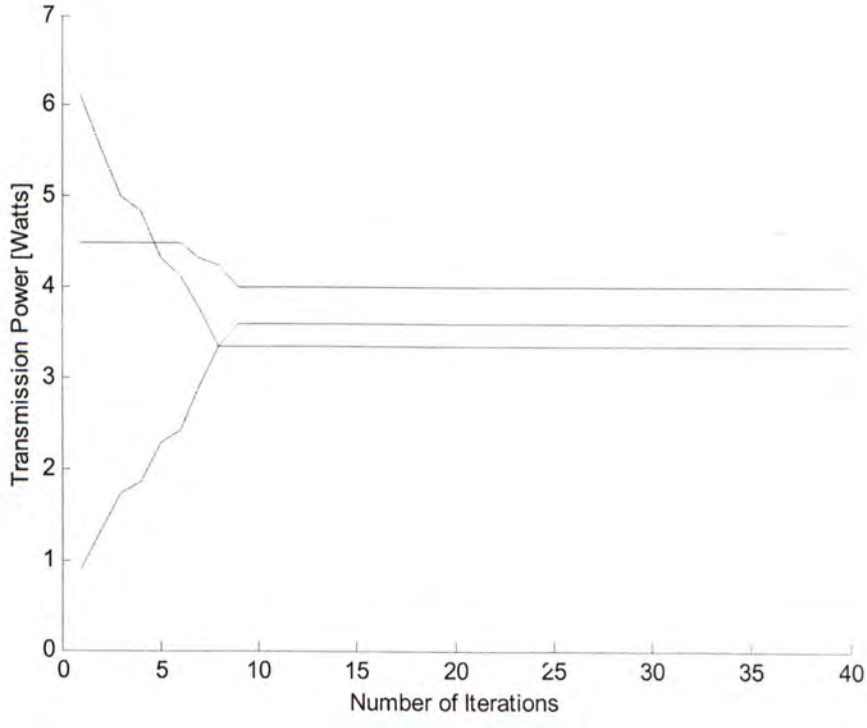

Figure 3.12 When the threshold $\xi = 0.1$, the convergence fails for PE Sectoring.

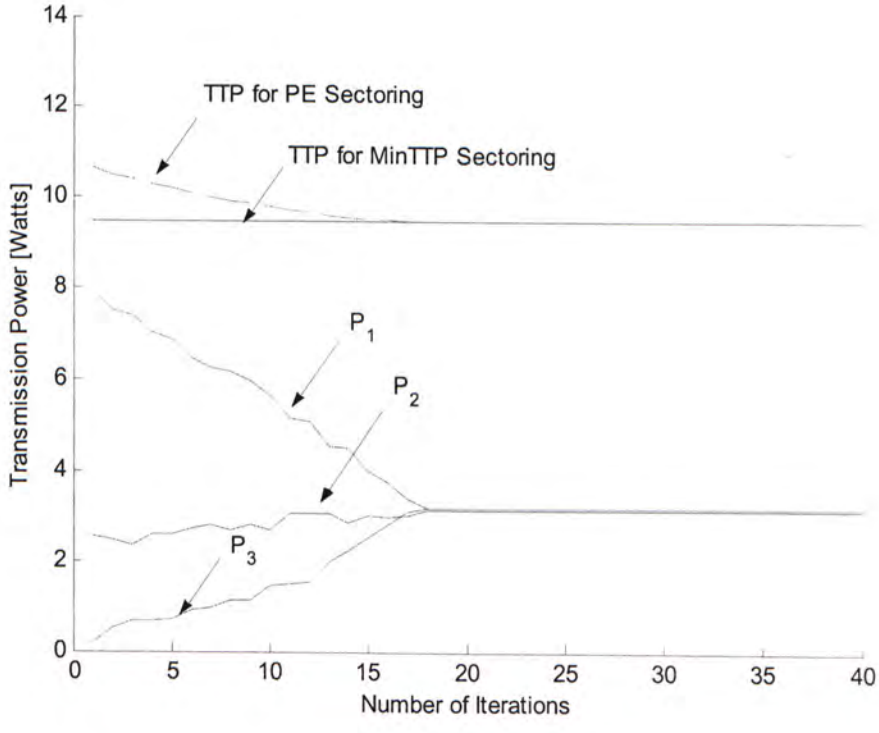

Figure 3.13 Comparison between MinTTP Sectoring and PE Sectoring in terms of TTP. Note the TTP for PE Sectoring converges to the optimal TTP by MinTTP Sectoring after 18 iterations.

Appendix

1. Dijkstra's Algorithm

- **DIJKSTRA**(G,w,S)

```
1   INITIALIZE-SINGLE-SOURCE (G,S)
2   S ← ∅
3   Q ← V[G]
4   while Q ≠ ∅
5       do u ← EXTRACT-MIN(Q)
6          S ← S ∪ {u}
7          for each vertex v ∈ Adj[u]
8              do RELAX(u,v,w)
```

- **INITIALIZE-SINGLE-SOURCE**(G,S)

```
1   for each vertex v ∈ V[G]
2       do d[v] ← ∞
3          π[v] ← NIL
4   d[S] ← 0
```

- **RELAX**(u,v,w)

```
1   if d[v] > d[u] + w(u,v)
2       then d[v] ← d[u] + w(u,v)
3            π[v] ← u
```

Note: $d[v]$: a shortest path length estimation from source s to vertex v

$\pi[v]$: the predecessor of v in a path

$w(u,v)$: the distance between u and v

EXTRACT-MIN(H): delete the node from heap H whose *key* (value) is minimum; returning a pointer the node.

2. Single-source Shortest Path algorithm in directed acyclic graphs

- **DAG-SHOREST-PATHS** (G,w,S)
  1. topologically sort the vertices of G
  2. INITIALIZE-SINGLE-SOURCE(G,S)
  3. **for** each vertex u taken in topologically sorted order
  4. **for** each vertex $v \in Adj[u]$
  5. **do** RELAX(u,v,w)

Chapter 4. Resectoring Algorithms

4.1. Introduction

After the dynamic sectoring (MinTTP or PE Sectoring), the interference is minimized or the load is balanced. However, when the distribution of the traffic changes, the previous "optimal" sectoring pattern would no longer be optimal. The cell sectoring structure is thus needed to adjust such that the system can maintain its optimal load distribution at all times. The question is when to resector the cell?

One method is to keep detecting the power load among the sectors, and resector the cell once the power changes. However, the received power from a fading channel changes very fast. It is not possible to resector the cell at the fading rate. If the power is averaged over a certain time interval (e.g. 20ms), the power varies smoothly. Usually, diversity techniques, such as RAKE receiver and multiple antennas are used to mitigate the fading effect. In this thesis, we only consider the static channel and no fading effect is taken into consideration. Therefore the power changes slowly.

Two resectoring schemes are discussed in this thesis. One is MinTTP Resectoring and the other is PE Resectoring. Both resectoring algorithms are based on the idea of *Nyquist Sampling Theorem* [35] to determine the resectoring interval. At the discrete time points, the base station detects the power change and readjusts the sector pattern when necessary.

4.2. Nyquist Sampling Theorem

Theorem 4.1 (*Nyquist Sampling Theorem*): Let $x(t)$ be a band-limited signal with $X(j\omega) = 0$ for $|\omega| > \omega_M$. Then $x(t)$ is uniquely determined by its samples $x(nT), n = 0, \pm 1, \pm 2, \cdots$, if

$$\omega_s > 2\omega_M \tag{4.1}$$

where $\omega_s = \frac{2\pi}{T}$.

Therefore, a continuously changing signal can be tracked by a discrete signal sequence with a fixed interval of $T = \frac{2\pi}{\omega_s}$. The smaller the T is, the higher the tracking accuracy can be achieved and a corresponding higher probing computation from (4.3) or (4.4) is needed.

4.3. MinTTP Resectoring

Suppose the power in sector k is $P_k(t)$. The total transmission power of the cell at time t is:

$$TTP(t) = \sum_{k=1}^{S} P_k(t) \tag{4.2}$$

At time points nT, the MinTTP (TTP_{MTTPS}) is calculated and compared to the TTP in the existing sector pattern. Resector the cell if the predefined the condition (4.3) is satisfied:

- ***MinTTP Resectoring Algorithm***

  Resector the cell, if:

  $$\frac{TTP(nT) - TTP_{MTTPS}}{TTP_{MTTPS}} > \xi, \qquad n = 0, 1, 2, \cdots \tag{4.3}$$

  where ξ is the threshold.

MinTTP Resectoring gives the optimal sectoring pattern at the each time point, however, each probing (4.3) has a computational complexity of $O(M^3S)$. Recall that the MinTTP Sectoring is based on the accurate location information. Too high complexity will induce the system non-real time, and therefore the power may not be kept at the minimum level.

4.4. PE Resectoring

At time points nT, compare the power of two neighboring sectors. If the difference exceeds the threshold, resector the cell using the following algorithm:

- ***PE Resectoring Algorithm***

  Resector the cell, if:

$$\sum_{k=1}^{S} I_k(nT) \geq 1, \qquad n = 0,1,2,\cdots \tag{4.4}$$

  where $I_k(t) = \begin{cases} 1, & \text{if } \frac{|P_k(t)-P_{k+1}(t)|}{P_k(t)} > \xi \\ 0, & \text{otherwise} \end{cases} \qquad k = 1,\cdots,S-1$

  and ξ is the threshold.

PE Sectoring has much less computational complexity, and real time resectoring can be expected.

4.5. Handoff

Resectoring will induce inter-sector handoff. Because of the spreading code reallocation, handoff brings with extra complexity for the system and yet may induce outage for a call. Thus a smaller handoff rate is preferred. The smaller the threshold ξ is, the more resectoring's happen and hence the more handoff will occur. However, a larger threshold will make the dynamic sectoring less efficient in reducing the interference. Therefore, it is

very important to select a proper resectoring threshold ξ to ensure the user's SIR while keep the handoff rate at a low level.

4.5.1. Handoff Load

After the MinTTP Resectoring, a new sector pattern is obtained. How to move the sectors from the previous sector pattern to the current one will produce different handoff load as shown in Figure 4.1. *Handoff Load* (L_{HO}) in this thesis is defined as the percentage of the users who are shifted away of their original sectors to others:

$$L_{HO} = \frac{\text{Number of users shifted from their original sectors}}{\text{Total number of users in the cell}} \tag{4.5}$$

MinTTP resectoring needs to compare L_{HO} for different sector move schemes before the spread code reallocation, and select the sector move scheme with the minimum handoff load.

In PE Resectoring, however, no such problem will occur, since during PE Resectoring, the sector boundaries move direction has already been determined in the PE Sectoring algorithm.

4.6. Performance

The simulation is based on a 2-D Poisson source model, i.e., if we assume that the traffic arrival obeys Poisson process and map the arriving mobiles into the cell with uniform distribution $f_{r,\theta}(r,\theta) = \frac{r}{\pi R^2}$, then the occurrence of the mobiles in the cell is a 2-D Poisson process.

Comparison of the average handoff load for MinTTP and PE Resectoring is shown in Table 4.1, where the handoff load increases when the threshold ξ increases, and the former Resectoring scheme has a lower handoff load than the latter. It is because the PE Resectoring may have more resectoring times. Meanwhile the "Ping-Pong" effect may also increase the handoff load.

Table 4.2 shows the average power for both resectoring schemes. Similar average power is obtained from both schemes. Increasing the threshold increases the average power in both schemes.

With a little more handoff load, and yet similar power transmitted, however much less complexity, PE Resectoring is more suitable for practical adoption than the MinTTP Resectoring.

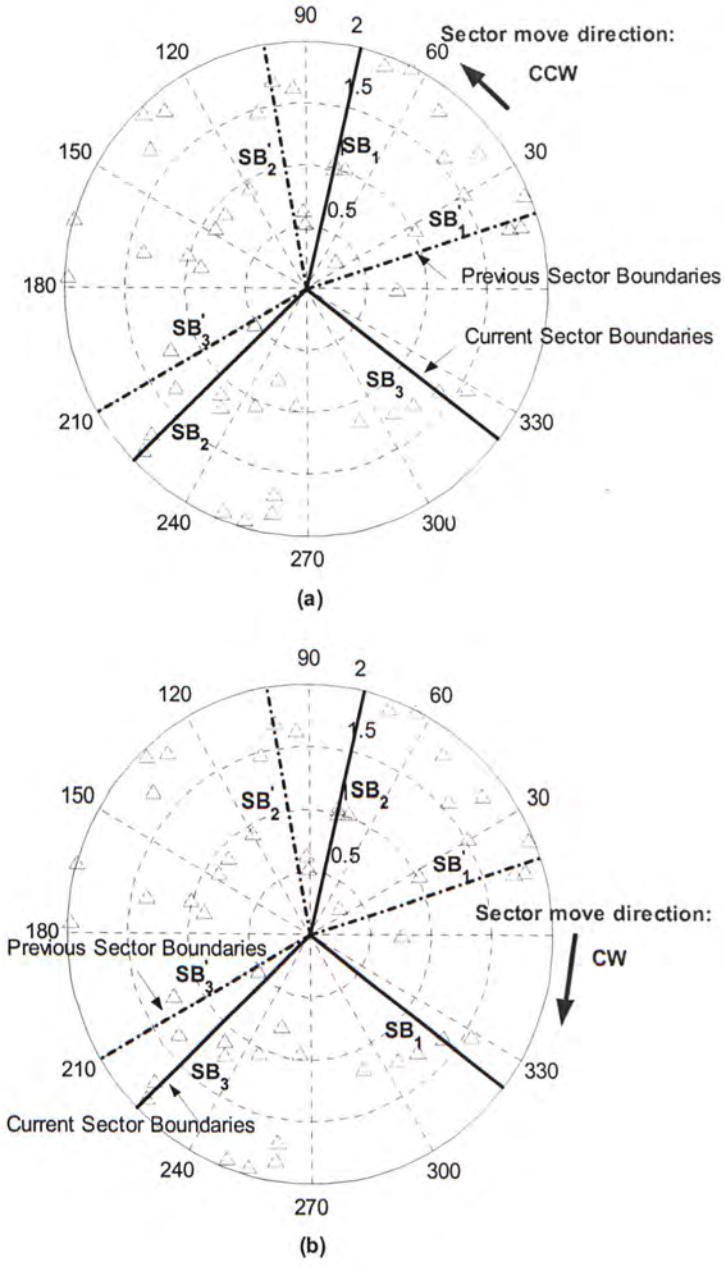

Figure 4.1 Different sector boundary move schemes will result in different handoff load. In (a) the handoff load is 0.8, while in (b) the handoff load is 0.26. Thus we select (b) as the solution due to its less handoff load.

Table 4.1 Average handoff load obtained from MinTTP and PE Resectoring

	Average Handoff Load	
	MinTTP Resectoring	PE Resectoring
$\xi = 0.02$	0.13	0.33
$\xi = 0.05$	0.09	0.24
$\xi = 0.1$	0.07	0.15

Table 4.2 Average power obtained from MinTTP and PE Resectoring [Watts], where the average number of mobile stations, $M = 30$, the number of sectors, $S = 3$, processing gain, $G = 19.3dB$, target SIR level, $\rho = 8.4dB$, VAF, $v = 0.479$, ORF, $\alpha = 0.2$, and thermal noise power $P_N = -103dBm$.

	Average Power [Watts]	
	MinTTP Resectoring	PE Resectoring
$\xi = 0.02$	6.27	6.49
$\xi = 0.05$	6.75	6.82
$\xi = 0.1$	6.94	7.05

Chapter 5. Conclusion and Future Work

5.1. Thesis Summary

Cell sectoring is used to reduce the co-channel interference so as to increase the system capacity. However, it works inefficiently when addressing hot-spot scenarios. Some congested sectors may induce outages, while the lightly loaded sectors may have spare capacity. Dynamic cell sectoring, i.e., adaptively changing the sector pattern according to the traffic can solve the problem.

In this thesis, we have studied the dynamic cell sectoring schemes for the CDMA cellular systems from three aspects: physical base, algorithms, and algorithm operations.

Beamforming techniques are discussed at the second chapter. Circular array is more suitable than linear array for sector beamforming because of its good lobe-shape persistence characteristic. A circular array BFN shown in Figure 2.6 can produce dynamic sector pattern with the aid of the Butler matrix, which is used to cancel the sidelobe effect.

It is shown that MinTTP Sectoring scheme gives the optimal sectoring pattern in polynomial complexity using a shortest path algorithm while suboptimal solution can be found using PE Sectoring with much less computational complexity. The relationship between MinTTP and PE sectoring is discussed under different scenarios. We find that PE Sectoring converges to MinTTP Sectoring.

Via detecting the traffic change and readjust the sector patterns, Resectoring algorithm ensures the system to keep its optimal load distribution at all times.

5.2. Future Work

In this thesis, perfect power allocation is assumed. If with no power control or imperfect power control, the sectoring criterion must be modified from the power to the SIR. Arbitrary sector size is assumed in the thesis. However, due to the finite number of array elements, the minimum sector size is $\frac{2\pi}{N}$, where N is the number of array elements. By adding this physical constraint, more efficient sectoring algorithms could be developed to bring the complexity further down.

Bibliography

[1] P. H. Lehne and M. Pettersen, "An overview of smart antenna technology for mobile communications systems", IEEE Communications Surveys, fourth quarter 1999, Vol.2 no.4

[2] D. Shim and S. Choi, " Should the smart antenna be a tracking beam array or switching beam array", Proc. IEEE VTC, Ottawa, May 1998

[3] M. Mahmoudi, et al, "Adaptive sector size control in a CDMA system using butler matrices", IEEE *International Conference on Communications* 1999, pp.1355-1359

[4] M. Mahmoudi and E. S. Sousa, "Joint Power Control, Base Station Assignment and Sectorization for CDMA Cellular Systems", VTC 2000, pp.573-580

[5] K. Gilhousen,et al, "On the Capacity of a Cellular CDMA System," IEEE Trans. on Vehicular Technology, Vol. 40, no. 2, pp.303-312, May 1991

[6] M. Ismail, et al, "Teletraffic performance of dynamic cell sectoring for mobile radio system", IEEE ICCS, Singapore, 1994, pp.1090-1094

[7] C. U. Saraydar and A. Yener, "Adaptive Cell Sectorization for CDMA Systems", IEEE Journal on Selected Areas in Communications, Vol. 19, no.6, June 2001

[8] K. Sipilä, et al, "Estimation of Capacity and Required Transmission Power of WCDMA Downlink Based on a Downlink Pole Equation", IEEE VTC2000, pp.1002-1005

[9] J. Wen, J. Sheu, and J. Chen, "An Optimal Downlink Power Control Method for CDMA Cellular Mobile Systems", IEEE *International Conference of Communications* 2001

[10] S. A. Grandhi, R. Vijayan, D. J. Goodman, J. Zander, "Centralized Power Control in Cellular Radio Systems", IEEE Transaction on Vehicular Technology, Vol.42, No.4, November 1993

[11] Q. Wu, " Performance of Optimal Transmitter Power Control in CDMA Cellular Mobile Systems", IEEE Transaction on Vehicular Technology, Vol. 48, No. 2, Mar 1999

[12] H. Holma and A. Toskala, *WCDMA for UMTS: Radio Access For Third Generation Mobiles Communications*, New York, John Wiley & Sons, 2000

[13] R. A. Monzingo and T. W. Miller, *Introduction to Adaptive Arrays*, New York, John Wiley & Sons, 1980

[14] J. E. Hudson, A*daptive array Principles*, IEE Electromagnetic Waves Series-11, 1981

[15] R. A. Horn and C. R. Johnson, *Matrices Analysis,* Cambridge University Press, 1987

[16] TD-SCDMA RTT for IMT-2000 Submission, 1998

[17] V. Kalinichev, "Analysis of Beam-steering and Directive Characteristics of Adaptive Antenna Arrays for Mobile Communications", IEEE Antennas and Propagation Magazine, Vol. 43, No.3, June 2001

[18] B. Sheleg, "A Matrix-Fed Circular Array for Continuous Scanning", Proceedings of IEEE, Vol.56, No.11, November 1968.

[19] G. L. St□er, *Principles of Mobile Communications,* Second Edition. Kluwer Academic Publisher, 2001

[20] T. S. Rappaport, *Wireless Communications Principles and Practice*, Prentice Hall, 1996

[21] J. S. Lee, L. E. Miller, *CDMA Systems Engineering Handbook*, Artech House, 1998

[22] K. I. Kim, *Handbook of CDMA System Design, Engineering, and Optimization*, Prentice Hall PTR, 2000

[23] J. C. Liberti, JR and T. S. Rappaport, *Smart Antennas for Wireless Communications: IS-95 and Third Generation CDMA Applications*, Prentice Hall, 1999

[24] G. V. Tsoulos, *Adaptive Antennas for Wireless Communications*, A Selected Reprint Volume, IEEE Press

[25] Z. Zhang and C. Douligeris, " Convergence of Synchronous and Asynchronous Greedy Algorithms in a Multiclass Telecommunications Environment", IEEE Transaction on Communications, Vol. 40, No. 8, August 1992

[26] S. Kandukuri and S. Boyd, "Optimal Power Control in Interference-Limited Fading Wireless Channels With Outage-Probability Specifications", IEEE Transaction on Wireless Communications, Vol. 1, No. 1, January 2002

[27] U. W. Pooch and J. A. Wall, *Discreet Event Simulation: A Practical Approach*, CRC Press, 1993

[28] S. Sahni, *Data Structures, Algorithms and Applications in C++*, McGraw Hill, 1998

[29] T. H. Cormen, C. E. Leiserson, R. L. Rivest, *Introduction to Algorithms*, The MIT press, 1990

[30] D. P. Bertsekas and R. Gallagar, *Data Networks*, 2nd ed. Englewood Cliffs, NJ: Prentice Hall, 1992

[31] R. C. Hansen, *Phased Array Antennas*, Wiley-Interscience Publication, 1998

[32] C. A. Balanis, *Antenna Theory: Analysis and Design*, Second Edition, John Wiley & Sons, 1997

[33] http://www.metawave.com/

[34] A. J. Viterbi, *CDMA: Principles of Spread Spectrum Communication*, Addison Wesley, 1995

[35] A. V. Oppenheim snd A. S. Willsky, *Signals and Sytems*, Second Edition, Prentice Hall, 1997.